

**The Dissolution Behavior of Ibuprofen and Griseofulvin in  
Bicarbonate Buffer Compared to Phosphate Buffer Using  
Intrinsic Dissolution Rate and Biphasic Dissolution**

By

**Saqer Alarifi**

A thesis submitted in partial fulfillment of the requirements for  
the degree of

Master of Science

In Pharmaceutical Sciences  
Faculty of Pharmacy and Pharmaceutical Sciences  
University of Alberta

## Abstract

In the small intestine, bicarbonate is the main buffering system to adjust the pH after the gastric emptying to pH 5.5-6.8. Bicarbonate gathered some attention to be used as a dissolution media to better mimic the in-vivo environment. However, evaporation of  $\text{CO}_{2(g)}$  interferes with the in vivo observed neutralization process. To maintain the pH,  $\text{CO}_{2(g)}$  must constantly added. In a previous study, they predicted based on the reaction kinetics that ibuprofen dissolution in 5 mM phosphate buffer will be equivalent to 10 mM bicarbonate buffer. However the dissolution of acidic drug will alter the pH of the phosphate media. The aim of the study was to investigate bicarbonate buffer compared to phosphate buffer as dissolution media for ibuprofen (IBU) and griseofulvin (GRI) with and without the use of bile salts, and to develop a method to test the similarity between dissolution of IBU 5 mM phosphate buffer and 10 mM bicarbonate buffer.

The intrinsic dissolution rate (IDR) was used to compare between dissolution of IBU and GRI in 10mM bicarbonate buffer (BCB) and phosphate buffer (PBS) with and without bile salts at pH  $6.8 \pm 0.05$ . The pH was monitored throughout the experiments. In case of bicarbonate,  $\text{CO}_{2(g)}$  was applied on the surface to control the pH rather than infused to avoid foaming. For IBU dissolution in 5 mM PBS a two compartment system was developed.

The IDR of IBU showed a significant difference between BCB and PBS without bile salts, which is in agreement with Krieg et al. GRI IDR showed a significant difference between PBS with bile salts and BCB with bile salts, where BCB was 83% higher than PBS. This indicates a difference in micelle shape in BCB compared to PBS which resulted in an enhanced solubilization. The similarity of the biphasic dissolution of IBU in PBS and BCB was rejected. Our study indicates the need of a better surrogate buffer to BCB, especially when large volumes are needed. The study also demonstrated the importance of testing bicarbonate buffer as dissolution media for class II drugs.

*Dedication*

*To my mother, my father, and myself*

## **ACKNOWLEDGEMENTS**

First and most thanks to god. Then to my supervisor Dr.Raimar Löbenberg for his kindness, guidance, advice, and continuous support. I cannot thank him enough for his endless help and motivation throughout my studies. And thanks to our lab manager Dr.Vijay Somayaji and my supervisors committee for their valuable comments and guidance. Also thanks to my current and past lab mats.

Finally, I would like to thank King Saud bin Abdulaziz University for Health Sciences, Saudi Cultural Bureau in Canada, and University of Alberta.

# TABLE OF CONTENTS

<b>Chapter 1: Introduction .....</b>	<b>1</b>
1.1 <i>In Vitro/In Vivo</i> Correlation .....	2
1.1.1 Physicochemical Factors .....	2
1.1.2 Physiological Factors .....	4
1.2 Bicarbonate Buffer .....	5
1.3 Biphasic Dissolution .....	7
1.4 Biopharmaceutical Classification System .....	10
1.5 Intrinsic Dissolution Rate .....	11
1.6 Rationale and Significance .....	12
1.7 Study Question .....	13
1.7 Aim of the Study .....	13
<b>Chapter 2: Methodology.....</b>	<b>15</b>
2.1 Intrinsic Dissolution Rate .....	16
2.1.1 Materials Used .....	16
2.1.2 Experiment Setup .....	16
2.1.3 Buffer Preparation .....	17
2.1.4 High Pressure Liquid Chromatography .....	18
2.1.5 Micelles Size .....	19
2.2 Biphasic Dissolution .....	20

2.2.1 Analytical Method .....	20
2.2.2 Franz Cell Biphasic Dissolution .....	20
2.2.3 Laminar Flow Biphasic Dissolution .....	21
2.2.3.1 Ibuprofen Partitioning.....	21
2.2.3.2 Ibuprofen Biphasic Dissolution .....	22
2.3 Statistical Analysis.....	23
<b>Chapter 3: Result .....</b>	<b>24</b>
3.1 High Pressure Liquid Chromatography Assay .....	25
3.2 Ibuprofen Intrinsic Dissolution Rate.....	26
3.2.1 Using 50 mM Phosphate Buffer .....	26
3.2.2 Using 10 mM Phosphate Buffer .....	27
3.2.3 Using 10 mM Bicarbonate Buffer .....	27
3.2.4 Using 50 mM Phosphate Buffer with Bile Salts.....	28
3.2.5 Using 10 mM Phosphate Buffer with Bile Salts.....	28
3.2.6 Using 10 mM Bicarbonate Buffer with Bile Salts.....	28
3.3 Griseofulvin Intrinsic Dissolution Rate .....	35
3.3.1 Using 10 mM Phosphate Buffer .....	35
3.3.2 Using 10 mM Bicarbonate Buffer .....	35
3.3.3 Using 10 mM Phosphate Buffer with Bile Salts.....	36
3.3.4 Using 10 mM Bicarbonate Buffer with Bile Salts.....	36

3.4 Two Compartment Biphasic Dissolution.....	43
3.4.1 IBU UV scan.....	43
3.4.2 Franz Cell Ibuprofen Biphasic Dissolution .....	43
3.4.3 Ibuprofen Biphasic Dissolution Using Laminar Flow Mixer.....	45
3.4.3.1 Partitioning of Ibuprofen.....	45
3.4.3.2 Ibuprofen Biphasic Dissolution .....	47
3.4.3.2.1 Biphasic Dissolution in 5 mM Phosphate buffer.....	47
3.4.3.2.2 Dissolution in 10 mM Bicarbonate Buffer .....	48
3.4.3.2.3 Biphasic Dissolution Profile Comparison .....	48
<b>Chapter 4: Discussion and Conclusion .....</b>	<b>53</b>
4.1 Intrinsic Dissolution Rate .....	54
4.1.1 Ibuprofen Intrinsic Dissolution Rate.....	54
4.1.2 Griseofulvin Intrinsic Dissolution Rate.....	57
4.2 Biphasic Dissolution .....	59
4.2.1 Franz Cell Biphasic Dissolution .....	59
4.2.2 Ibuprofen Biphasic Dissolution Using Laminar Flow Mixer.....	60
4.2.2.1 Partitioning of Ibuprofen.....	61
4.2.2.2 Ibuprofen Biphasic Dissolution .....	61
4.2.2.2.1 Dissolution in 5 mM Phosphate Buffer .....	61
4.2.2.2.2 Dissolution in 10 mM Bicarbonate Buffer .....	62



4.2.2.2.3 Biphasic Dissolution Profile Comparison .....	62
4.3 Conclusion .....	63
4.4 Limitations .....	65
4.5 Future Directions.....	65
References.....	66

### **List of Figures**

Figure 2.1	IDR experimental design while monitoring pH. The experimental conditions (disk speed, flow rate, time) were adjusted to produce measurable concentrations and a linear relationship for each drug.	19
Figure 2.2	Illustration of biphasic dissolution using of Franz cells. Octanol phase (yellow) in Franz cells, buffer (blue) in main vessel, with IBU (white), being stirred at 100 rpm, with the media circulated at 5 mL/min. A hydrophilic membrane filter (red) was used	22
Figure 2.3	Illustration of the biphasic dissolution setup with the use of a stirrer. Octanol phase yellow, buffer blue in Vessel B.	23

The medium was pumped at 10 mL/min between Vessels A and B.

- Figure 3.1 Standard curve for IBU. The error bars represent the mean  $\pm$  upper and lower limits (n=2). 26
- Figure 3.2 Figure 3.2: Standard curve for GRI. The error bars represent the upper and lower limits (n=2). 26
- Figure 3.3 The effects of buffer strength and composition on the cumulative amount of dissolved of IBU (mg) at a speed of 100 rpm, and at 37°C, the disk was compressed at a force of 1,000 psi. The linear trend estimation is shown as a dotted line. The error bars represent the mean  $\pm$  SD (n=3). 30
- Figure 3.4 The effects of buffer strength, composition, and surfactant on the IBU IDR in mg/min.cm<sup>2</sup>. The IDR was calculated by dividing the slope by the disk area (0.5 cm<sup>2</sup>). The error bars represent the mean  $\pm$  SD (n=3). 31
- Figure 3.5 The effect of buffer strength and composition on pH in the presence of IBU. The error bars represent the mean  $\pm$  SD (n=3). 32
- Figure 3.6 The effect of buffer strength, composition, and surfactant on the cumulative amount of IBU dissolved (mg). at a speed 33

of 100 rpm, and 37°C, where the disk was compressed with a force of 1000 psi. The linear trend estimation is shown as a dotted line. The error bars represent the mean  $\pm$  SD (n=3).

Figure 3.7 The effect of buffer strength, composition, and surfactant on pH. The error bar represent the mean  $\pm$  SD (n=3). 34

Figure 3.8 The effects of buffer composition and surfactant on cumulative GRI dissolved ( $\mu\text{g}$ ). at a speed of 200 rpm, and 37°C, the disk was compressed at a force of 4000 psi, The linear trend estimation is shown as a dotted line. The error bars represent the mean  $\pm$  SD (n=3). 38

Figure 3.9 The effects of buffer composition and surfactant on the GRI IDR in  $\mu\text{g}/\text{min}\cdot\text{cm}^2$ . The IDR was calculated by dividing the slope by the disk area ( $0.5\text{ cm}^2$ ). The error bars represent the mean  $\pm$  SD (n=3). 39

Figure 3.10 The effect of buffer composition on pH. The error bar represent the mean  $\pm$  SD (n=3). 40

Figure 3.11 The effect of buffer composition on cumulative dissolved GRI ( $\mu\text{g}$ ). at speed of 200 rpm, and 37°C, where the disk was compressed at force of 4000 psi, The linear trend 41

estimation is shown as a dotted line. The error bars represent the mean  $\pm$  SD (n=3).

Figure 3.12 The effect of buffer composition on pH. The error bar represent the mean  $\pm$  SD (n=3). 42

Figure 3.13 Average diameter (nm) of bile salts micelles in 10 mM BCB and 10 mM PBS. The error bars represent the upper and lower limits (n=2). 43

Figure 3.14 Cumulative % dissolution of IBU using a mixer, with 200  $\mu$ g/mL IBU (250 mL 5 mM PBS), 50 mL octanol (Octa), and the total percentage dissolved (paddle speed 100 rpm, laminar mixer speed 75 rpm, at 37°C). The error bars represent the upper and lower limits (n=2). 45

Figure 3.15 IBU dissolution medium pH (primary y axis), and concentration of IBU dissolved mg/mL (secondary axis), using Franz cells. The error bars represent the mean  $\pm$  SD (n=3). 46

Figure 3.16 Cumulative % dissolution of IBU using a mixer; 200  $\mu$ g/mL IBU (250 mL 5 mM PBS), 50 mL octanol (Octa), and total percent dissolved (paddle speed 100 rpm, laminar mixer 47

speed 75 rpm, at 37°C). The error bars represent the upper and lower limits (n=2).

Figure 3.17 IBU buffer dissolution medium pH (primary y axis) and concentration of IBU mg/mL (secondary axis) over time, using a mixer. The error bars represent the mean  $\pm$  upper and lower limits (n=2). 48

Figure 3.18 Cumulative % dissolution in 5 mM PBS using a mixer; 250 mL of 5 mM PBS, 50 mL of octanol (Octa), and total percent dissolved (paddle speed 100 rpm, mixer speed 75 rpm, at 37°C). The error bars represent the mean  $\pm$  SD (n=3). 50

Figure 3.19 PBS medium pH (primary y axis) and concentration of IBU mg/mL (secondary axis) over time, using a mixer. The error bars represent the mean  $\pm$  SD (n=3). 51

Figure 3.20 IBU biphasic cumulative dissolution percentage in 10 mM BCB using a mixer; 250 mL of 10 mM BCB, 50 mL octanol (Octa), and total percent dissolved (100 rpm, mixer speed 75 rpm, at 37°C). The error bars represent the mean  $\pm$  SD (n=3). 51

Figure 3.21 BCB medium pH (primary y axis) and concentration of IBU 52  
mg/mL (secondary axis) over time, using a mixer. The error  
bars represent the mean  $\pm$  SD (n=3).

## List of Tables

Table 1.1:	Drug examples and their BCS classes.	12
Table 3.1:	P values for the IBU IDR in different media, using the two-tailed t test; *indicates a significant difference.	35
Table 3.2:	P values for the GRI IDR in different media, using the two-tailed t test. *Indicates a significant difference.	43
Table 3.3:	MMIP and similarity factor ( $f_2$ ) between the buffers, octanol, and total cumulative percent dissolved using biphasic dissolution with a mixer. A is accepted similarity, R is rejected similarity.	53
Table 3.4:	P values for the biphasic dissolution using a mixer for 5 mM PBS and 10 mM BCB, using a two-tailed t test. *Indicates a significant difference.	53

## List of Abbreviations

A	Surface area
AUC	Area under the curve
BBBS	Bicarbonate buffer with bile salts
BCB	Bicarbonate buffer
BCS	Biopharmaceutical classification system
° C	Celsius degree
C <sub>b</sub>	Substance concentration
cm	Centimeter
cm <sup>2</sup>	Centimeter square
CMC	Critical micelles concentration
CO <sub>2</sub>	Carbon dioxide
C <sub>s</sub>	Substance solubility
D	Diffusion coefficient
dm	Change in amount of drug dissolved
dt	Change in time
e.g.	For example
EMA	European Medicines Agency
Eq	Equation
f <sub>2</sub>	Similarity factor



FaSSIF	Fasted State Simulated Intestinal Fluid
FaSSIF V2	Fasted State Simulated Intestinal Fluid second version
g	Grams
GI	Gastrointestinal
GRI	Griseofulvin
h	Diffusion layer thickness
H <sup>+</sup>	Proton
H <sub>2</sub> CO <sub>3</sub>	Carbonic acid
H <sub>2</sub> O	Water
HCl	Hydrochloric acid
HCO <sub>3</sub> <sup>-</sup>	Bicarbonate
HPLC	High pressure liquid chromatography
hr	Hours
Ibu	Ibuprofen
IDR	Intrinsic dissolution rate
IVIVC	Invitro-invivo correlation
k <sub>0</sub>	Zero order dissolution constant
K <sub>a</sub>	Intestinal absorption rate constant
k <sub>a</sub>	Ionization factor
M	Molar

MAD	Maximum absorbable dose
mg	Milligrams
μg	Micrograms
min	Minutes
mL	Milliliter
mm	Millimeter
mM	Millimolar
MMIP	Multivariate model independent procedure
N	Normal
NaOH	Sodium hydroxide
nm	Nanometer
PBBS	Phosphate buffer with bile salts
PBS	Phosphate buffer
PTEF	Polytetrafluoroethylene
psi	Pound-force per square inch
R <sup>2</sup>	Coefficient of determination
Rec.	Reaction
rpm	Round per minute
S	Solubility
S <sub>a</sub>	Surface area

SD	Stander deviation
SITT	Small intestines transits time
SIWV	Small intestines water volume
USFDA	United State Food and Drug administration
USP	United State pharmacopeia
uv	Ultra-violet
WHO	World health organization

# **Chapter One**

## **Introduction**

## 1. Introduction

### 1.1. *In Vitro/In Vivo* Correlation

The US Food and Drug Administration (USFDA) defines an *in vitro/in vivo* correlation (IVIVC) as being a mathematical tool for describing the relation between *in vitro* data (e.g., dissolution) and its *in vivo* response. The ability to predict the pharmacokinetics of a drug means fewer *in vivo* studies are needed, which leads to lower development costs, time savings, and avoiding unnecessary biostudies. For these reasons, and with an increase in confidence in *in vitro* methods, the USFDA reported that the percentage of IVIVCs between 1982 and 1992 was only 15%, with this number increasing significantly to 75% in 1994.<sup>1</sup>

To do so, multiple physicochemical, physiological, and biopharmaceutical factors should be taken into account.

#### 1.1.1. Physicochemical Factors

Physicochemical properties of drugs play an important role in the determination of an IVIVC, as almost all orally-delivered drugs need to dissolve in order to be absorbed in the GI tract; however, dissolution depends on several factors, such as solubility, pH, particle size, and salt formation. One of the best-known attempts to model dissolution is the Noyes–Whitney equation:

$$\frac{dm}{dt} = \frac{DS_a(C_s - C_b)}{h} \quad \text{Eq. 1.1}$$

where  $dm/dt$  is the amount of dissolved substance in time  $t$ ,  $D$  is the diffusion coefficient of the substance in the diffusion layer,  $S_a$  is the surface area of the substance,  $C_s$  is solubility, where  $C_b$  is the substance concentration in the bulk medium, and  $h$  represent the diffusion layer thickness. When sink conditions are assumed,  $C_b$  will be equal to zero, giving:

$$\frac{dm}{dt} = \frac{DS_aC_s}{h} \quad \text{Eq. 1.2}$$

As seen from Eq. 1.2, the drug dissolution rate is dependent on its solubility.

The Noyes–Whitney equation cannot be applied in a clinical setting, however, as the equation does not take certain factors, such as the effects of pH and transit time, into account.<sup>2</sup> In an attempt to find a clinically applicable model, the maximum absorbable dose was developed by Johnson and Swindell:

$$MAD = SKa \times SITT \times SIWV \quad \text{Eq. 1.3}$$

where  $MAD$  is the maximum absorbable dose,  $S$  is the solubility,  $K_a$  is the intestinal absorption rate constant,  $SITT$  is the small intestine transit time, and  $SIWV$  is the small intestine water volume. Solubility is usually measured at pH 6.5, with  $SIWV$  being 250 mL, and  $SITT$  assumed to be 3 hr. This approach has many limitations, however, and is only used for initial assessments.<sup>3</sup>

For a more comprehensive approach, all the physicochemical properties should be considered. Particle size is another significant factor; a reduction in particle size increases the effective surface area, leading to an increase in solubility.

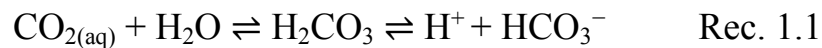
The ionization factor of the drug ( $k_a$ ), or its logarithmic value ( $pK_a$ ), is also a critical factor. It is known that the ionized form is more soluble than the non-ionized form. To account for the ionization, the pH gradient throughout the GI tract should be considered. The complexity of these factors makes it difficult to build an accurate dissolution model.<sup>4</sup>

### **1.1.2. Physiological Factors**

Physiological conditions can affect a drug on many levels; for instance, dissolution, and the absorption rate and extent. In some cases, a drug needs to be ionized in order to dissolve it, which is affected by the pH of the dissolution medium. The pH profile of the GI tract ranges from pH 1–2 in the stomach to pH 7–8 in the colon, and pH 6–8 in the small intestine. Therefore, pH changes can not only affect dissolution, they can also change the permeability of a drug. Besides pH, secreted surfactants, mainly bile salts, can also affect solubility; the rate of bile secretion ranges from 0.2 mL/min to 4 mL/min in the digestion state. Another factor affecting a drug in the GI tract is transit time, which can affect the rate and extent of absorption of the drug. For a successful IVIVC, these factors need to be taken into account.<sup>5–7</sup>

## 1.2. Bicarbonate Buffer

In the small intestine, bicarbonate ( $pK_a=6.5$ ) is the main buffer that adjusts the pH (to 5.5–6.5) after gastric emptying has occurred. It is secreted from the pancreas and lumen epithelial cells at concentrations ranging from 9–20 mM. Bicarbonate ( $\text{HCO}_3^-$ ) reacts with an acidic proton ( $\text{H}^+$ ) to give carbonic acid ( $\text{H}_2\text{CO}_3$ ), which undergoes dehydration to give water ( $\text{H}_2\text{O}$ ) and aqueous carbon dioxide ( $\text{CO}_2$ ), and this reaction is reversible (Rec. 1.1).<sup>8</sup>



In attempt to simulate the gastrointestinal (GI) buffering system, in terms of buffer species and capacity, bicarbonate has attracted some attention for use as a dissolution medium. A better correlation with the *in vivo* environment is obtained, but maintaining the pH is a major drawback, due to the escape of  $\text{CO}_{2(\text{g})}$ . To maintain the pH level,  $\text{CO}_{2(\text{g})}$  must be supplied to stabilize the dissolved  $\text{CO}_2$  fraction, which leads to an adjustment in  $\text{H}_2\text{CO}_3$  and  $\text{HCO}_3^-$  concentrations, according to the Henderson–Hasselbalch equation.<sup>9,10</sup> Fadda *et al.* reported three successful methods for maintaining constant  $\text{CO}_2$  levels, by: 1) continuous sparging of  $\text{CO}_2$  into the system; 2) applying a mineral oil layer on the surface; or 3) sealing the vessel completely.<sup>8</sup>



In their study, McNamara *et al.* used bicarbonate buffers (BCBs) at pH 5.0 and 6.8 for the intrinsic dissolution of indomethacin and dipyridamole, as examples of low-solubility acidic and basic drugs. They used 5%, 10%, and 20% CO<sub>2</sub> to adjust the pH with 1 N sodium hydroxide (NaOH) at room temperature, and assumed that equilibrium was achieved after 30–40 min. After transfer of the medium to the dissolution vessel, the medium was sparged with CO<sub>2</sub> to compensate for any loss during the transfer, and the pH was adjusted with 1N NaOH. CO<sub>2</sub> was supplied to the dissolution medium throughout the experiment. They recommended the use of CO<sub>2</sub> to establish the BCB used as a dissolution medium, while the CO<sub>2</sub> supply during the experiment mimicked a continuous *in vivo* supply of bicarbonate;<sup>9</sup> however, due to the thermal stability, estimation of equilibrium time and, most importantly, bubble formation, this method showed poor reproducibility.<sup>10,11</sup>

In an effort to avoid bubble formation and reduce costs, Boni *et al.* modified the method of preparation of the bicarbonate medium. They used a constant concentration of NaOH, sparged with CO<sub>2</sub> at a flow rate of 400 mL/min, until pH 6.5 was achieved, in approximately 20 min at 37±0.5°C. Constant CO<sub>2</sub> was supplied above the medium to avoid bubble formation. They concluded that the use of bicarbonate as a dissolution medium is impractical due to its instability, poor reproducibility, and time consumption. Also, the used of biorelevant media (e.g.,

Fasted State Simulated Intestinal Fluid – FaSSIF) was difficult due to the significant foam formation and time frame (approximately 3 hr).<sup>10</sup>

Liu *et al.* used a modified Hanks' buffer to test the ability of a physiological BCB to discriminate between different enteric coating polymers. They prepared the buffer by purging CO<sub>2(g)</sub> into Hanks' buffer to obtain a pH of 6.8. The CO<sub>2</sub> was supplied 2 cm under the dissolution medium surface at a low flow rate in order to maintain the desired pH and to avoid bubble formation. The modified Hanks' buffer was reproducible and discriminative between the different polymers, whereas the phosphate buffer (PBS) failed.<sup>11</sup>

Sheng *et al.*<sup>12</sup> compared the intrinsic dissolution rate (IDR) of Biopharmaceutical Classification System (BCS) class II drugs using bicarbonate and phosphate buffers. The BCB was prepared by purging CO<sub>2</sub> into 15 mM sodium chloride. They found that the PBS IDR was at least 30% higher than the bicarbonate IDR, indicating that more studies are needed to assess the correlation of bicarbonate and US Pharmacopeia (USP) PBS. Krieg *et al.*<sup>13</sup> proposed a lower strength PBS (4–8 mM) be used as surrogate for the BCB in Ibuprofen (IBU) dissolution.

### **1.3. Biphasic Dissolution**

Conventional dissolution is a standard procedure that tests the quality of drug products; however, dissolution profiles do not represent actual *in vivo* data, especially for low-solubility molecules. A new method that correlates better with *in*

*vivo* dissolution is needed. One concept missing from conventional dissolution is an organic sink.<sup>14</sup>

In 1961, Wurster and Polli showed the effects of adding norite as an adsorbent in the dissolution of benzoic acid. The experiment exhibited a linear dissolution profile for benzoic acid.<sup>15</sup> Doluisio and Swintosky then developed a rocking apparatus, where an inverted V-shaped glass was used. One tube was filled with the drug dissolved in a low-pH buffer, whilst the other tube was filled with a free buffer, and cyclohexane was used as a barrier between the two buffer systems. They recommended the use of this system to obtain a constant dissolution of the drug, whereby the constant removal of the drug from one buffer gave an advantage over the saturated dissolution medium.<sup>16</sup> An *in vivo* absorption correlation was not established, however, until Levy *et al.* showed that the dissolution of salicylic acid could be correlated with *in vivo* pharmacokinetics, although this relationship was established with relatively water-soluble drugs.<sup>17</sup> In 1967, Niebergall *et al.* reported the first use of a biphasic dissolution system, with octanol and a buffer in one vessel; when they tested whole tablets, the aqueous steady state was lower than the saturation concentration.<sup>18</sup> This reports focused attention on the idea of removing the drug from the aqueous phase to simulate an *in vivo* environment.

Later, the concept of a sink condition was introduced, in which the dissolution medium contained only 20% of the maximum solubility of the drug.<sup>19,20</sup> A lot of

effort was made to maintain a sink condition, especially in the case of low-solubility drugs. Introducing a surfactant into the dissolution medium demonstrated the ability to maintain a sink condition; however, the presence of a high molar concentration of surfactant could interfere with the dissolution process.<sup>21,22</sup> Another way to maintain a sink condition, is the use of co-solvents, wherein a miscible organic solvent is used with the dissolution medium. This method does not reflect any *in vivo* environment, however, and also the organic solvent interferes with the dissolution of the drug in the buffer.<sup>23,24</sup> A flow-through cell (USP apparatus IV) could be used to maintain a sink condition when an open loop system is used, but this method comes at a high cost, as a large volume of dissolution medium is required in order to dissolve low-solubility drugs.<sup>25-27</sup>

One of the most successful approaches for simulating sink conditions is the use of immiscible organic solvents with the dissolution medium. In many studies, biphasic dissolution has been used because of its simplicity, capability, and ability to simulate *in vivo* conditions. The biphasic system avoids the use of abnormal solutes, such as surfactants, or the use of meaningless solvents, and is, at the same time, a practical method. The organic layer acts as a reservoir for low-solubility drugs, which it can constantly partition. Also, octanol acts similarly to a lipid membrane, as it has a long alkyl, hydrophobic, and polar hydroxyl group; however, the speed and design of the experiment need to be well thought out in order to avoid

any mixing of the two phases, where the octanol could form an emulsion, as the drug could be partitioned into the octanol emulsion, rather than dissolving in the buffer, then partitioning into the octanol.<sup>28-33</sup>

#### **1.4. Biopharmaceutical Classification System**

The BCS divides drugs into four groups (as it shown in Table 1.1) based on their solubility, dissolution, and permeability.<sup>34</sup> A drug is considered to be highly soluble when the highest drug strength is soluble in 250 mL at 37°C, pH of 1-6.8 as per United States Food and Drug Administration (USFDA), 1-8 as per European Medicines Agency (EMA), or 1.2-6.8 according to World Health Organization (WHO).<sup>35-37</sup> The number of pH used, depends on the drug's pKa. Shake flask method is usually used, where the drug is incubated with the solvent in a covered flask for 48 h to 2 weeks, then the drug concentration in the solvent is analyzed to determine its maximum solubility. Other methods can be used if appropriate justification is given.

A drug is considered to be highly orally permeable when 85% or more of an administered dose is absorbed, compared to its intravenous reference dose. Usually, this is determined by pharmacokinetic studies, suitable animal models, or *in vitro* methods, such as Caco-2 cells. The USFDA considers a drug to have been rapidly dissolved when >85% of the product is dissolved within 15 min in 900 mL or less

dissolution medium, using USP apparatus I at 100 rpm (or 50 rpm using apparatus II), and rapidly dissolved when >85% of the product is dissolved within 30 min.

### 1.5. Intrinsic Dissolution Rate

The IDR is a method developed by Wood, wherein the pure substance dissolution rate is measured using a constant surface area. There are two types of IDR apparatus that have been adapted by different regulatory agencies, one being the rotating dissolution disk, and the other the static dissolution disk; the latter is only mentioned in the USP.<sup>38,39</sup> The IDR apparatus consists of a steel punch and die with a diameter of 0.2–1.5 cm. The test material is compressed in the die, then the die is transferred to a dissolution vessel and attached to a stirrer.<sup>20</sup> There have been attempts to modify the apparatus; for instance, a miniaturized rotating disk has been developed in which a lesser amount of test material is needed. This is important for early screening in drug development.<sup>40–43</sup> The IDR is determined by plotting the linear relationship between drug dissolved and time:

$$IDR = \frac{dm}{dt} \frac{1}{A} \quad \text{Eq. 1.4}$$

,where the unit of the IDR is mg/min/cm<sup>2</sup>,  $dm$  is the change in drug dissolved (mg),  $dt$  is the change in time (min), and  $A$  is the surface area of the die (cm<sup>2</sup>).

Yu *et al.* studied the feasibility of the IDR to be used to classify drugs and the effects of various experimental variables. The IDR was recommended to be used in

BCS rather than solubility, as the IDR is a rate phenomenon, which correlates closer with *in vivo*, as opposed to maximum phenomena. Also, the IDR has proven to be robust, as compression pressure, die position, and dissolution volume does not affect the IDR. Yu *et al.* proposed 0.1 mg/mL.cm<sup>2</sup> to be the cut-off limit for classifying drugs as highly soluble, with a 2000 psi compression pressure, 900 mL dissolution medium, and 100 rpm, with the die being 0.5 inch from the bottom of the vessel. The relationship between the IDR and solubility need to be investigated further. A drug is considered to be highly soluble when the maximum dose is soluble in 250 mL aqueous medium, but the maximum dose does not factor in the IDR.<sup>44</sup>

Table 1.1: Drug examples and their BCS classes.

<b>Class</b>	<b>Solubility</b>	<b>Permeability</b>	<b>Example</b>
<b>Class I</b>	High	High	Verapamil
<b>Class II</b>	Low	High	Ibuprofen
<b>Class III</b>	High	Low	Atenolol
<b>Class IV</b>	Low	Low	Ciprofloxacin

## **1.6.Rationale and Significance**

The selection of the dissolution medium is one of the most important factors to be considered when establishing an IVIVC. The type of medium chosen and strength

affect the dissolution behavior of the drug. The reaction kinetics of BCB can result in different dissolution behaviors of low-solubility drugs. Furthermore, the reaction kinetics will affect the aggregation of bile salts, as the bile salts aggregation process is affected by ion concentration and type. Also, adding CO<sub>2</sub> on the surface of the dissolution medium will help to maintain a constant pH without bubble formation and disruption to the hydrodynamics in the dissolution vessel.

This is particularly important in the case of class II drugs, where the dissolution is the rate limiting step. Dissolution differences observed between BCB and PBS could enhance the *in vivo* understanding of the dissolution of low soluble drugs.

### **1.7. Study Question**

Is there a difference in the dissolution behavior of acidic and neutral BCS class II drugs in bicarbonate vs. phosphate buffer?

### **1.8. Aims of the Study**

- To compare a BCB to a PBS as dissolution media for IBU and GRI, with and without the use of bile salts.
- To develop a suitable method for adding CO<sub>2</sub> to the media without affecting the hydrodynamics to maintain the pH of the test medium.



- To develop a biphasic dissolution system to test the similarity of IBU dissolution profile in a 5 mM PBS and in a 10 mM BCB without altering the pH of the media.

# **Chapter Two**

## **Methodology**

## **2. Methodology**

### **2.1. Intrinsic Dissolution Rate**

#### **2.1.1. Materials Used**

Ibuprofen (IBU) was purchased from Medisca (QC, Canada), griseofulvin (GRI) from ICN biomedical (Ohio, USA), lecithin from Alfa Aesar (Massachusetts, USA), sodium taurocholate from Calbiochem (Massachusetts, USA), potassium dihydrogen phosphate from Fisher Scientific (New Jersey, USA), sodium bicarbonate and sodium hydroxide from Caledon Laboratories (Ontario, Canada), and o-phosphoric acid and octanol from Fisher Chemical (New Jersey, USA)

#### **2.1.2. Experimental Setup**

An 8 mm disk was compressed into a tablet die at 2,000 psi for IBU and 4,000 psi for GRI, for 1 min, using a Carver hydraulic press (Wisconsin, USA). Then, the surface of the disk was gently cleaned using a Kimwipe to remove any loose particles.

For IBU, 50 mL of 0.001 M hydrochloric acid (HCl) was placed into a jacketed vessel and warmed to 37°C. The buffer was injected at 2.5 mL/min over 20 min, with the disk speed at 100 rpm, as shown in Figure 2.1. Samples of 2 mL were taken at 5, 10, 15, and 20 min, then filtered through a 0.2 µm pore-size polytetrafluoroethylene (PTFE) syringe filter (Fisher Scientific, China).

For GRI, 50 mL of 0.001 M HCl was placed into a jacketed vessel and warmed to 37°C. The buffer was injected at 0.208 mL/min over 120 min at 200 rpm. Samples of 2 mL were taken at 30, 60, 90, and 120 min, then filtered through a 0.2 µm pore-size PTEF syringe filter (Fisher Scientific, China).

### **2.1.3. Buffer Preparation**

The initial buffer concentrations were measured to be 10 mM, after dilution with the HCl in the media at the end of the experiment. The pH was monitored by an Orion 520A pH meter (Orion Research Inc., Massachusetts, USA).

For IBU, 1.68 g of sodium bicarbonate was dissolved in 1000 mL deionized water, then the pH was adjusted to 6.8 by sparging CO<sub>2(g)</sub> onto the surface of the buffer. The buffer concentration was verified before and after the experiment by using a Thermo Scientific Orion Carbon Dioxide Electrode (Thermo Fisher Scientific, Massachusetts, USA) connected to an Accumet AB250 pH/mV/ion meter (Fisher Scientific, Massachusetts, USA). Amounts of 2.72 g and 6.8 g of potassium dihydrogen phosphate, in 1000 mL of deionized water, were used for 10 mM and 25 mM phosphate buffers, then the pH was adjusted with NaOH to pH 6.8. Sodium taurocholate (6 mM) and lecithin (0.4 mM) were added to the buffer to simulate bile salts, when needed. Samples of 2 mL were taken at 5, 10, 15, and 20 min.

For the GRI dissolution, 2.52 g of sodium bicarbonate was dissolved in 1000 mL deionized water, then the pH was adjusted to 6.8 by sparging CO<sub>2(g)</sub> onto the surface of the buffer, the concentration was verified using the electrode described above. Where 4.08 g of potassium dihydrogen phosphate in 1000 mL of deionized water was used for the 10 mM phosphate buffer, the pH was adjusted to pH 6.8 using NaOH. Sodium taurocholate (9 mM) and lecithin (0.6 mM) were added to the buffer to simulate bile salts, when needed.

#### **2.1.4. High-Pressure Liquid Chromatography**

High-pressure liquid chromatography (HPLC) was used to analyze the dissolution of IBU and GRI. An LC-600 Shimadzu pump was used (Shimadzu, Japan), connected to an 851-AS Jasco autosampler (Tokyo, Japan) and a UV-957 Jasco UV detector (Tokyo, Japan). A LiChrospher 100 reverse phase-18 (Merck, Darmstadt, Germany), with a 5 µm particle size, was used for both drugs. The data were processed using Clarity v. 7.0 (DataApex Ltd., Czech Republic).

For IBU, a modified HPLC method from Jahan et al. was used, C18 column with a 0.7 mL/min flow rate, an injection volume of 10 µg, and UV detection at 222 nm, and a run time of 15 min. The mobile phase was prepared by dissolving 1.75 g of dibasic potassium hydrogen phosphate in 1000 mL of water added to acetonitrile at 1:1, then the pH was adjusted to  $6.0 \pm 0.05$  with concentrated ortho-phosphoric

acid or sodium hydroxide. The mobile phase was then filtered and degassed. All the chemicals were HPLC grade. The retention time was 8 min.<sup>45</sup>

For GRI, a modified HPLC method, from Trotta et al., was used, C18 column with a 0.6 mL/min flow rate and 40  $\mu$ g injection volume. The sample was detected at 245 nm with a run time of 10 min. The mobile phase was prepared by mixing methanol to water at 7:3. Then, the mobile phase was filtered and degassed.<sup>46</sup> All the chemicals were HPLC grade. The peak retention time was 5 min.

### 2.1.5. Micelle Size

The average diameter and size distribution of the bile salts micelles in the phosphate and BCBs were estimated by a dynamic light-scattering technique, using a Malvern Zetasizer™ 3000 (Malvern Instruments Ltd., UK).

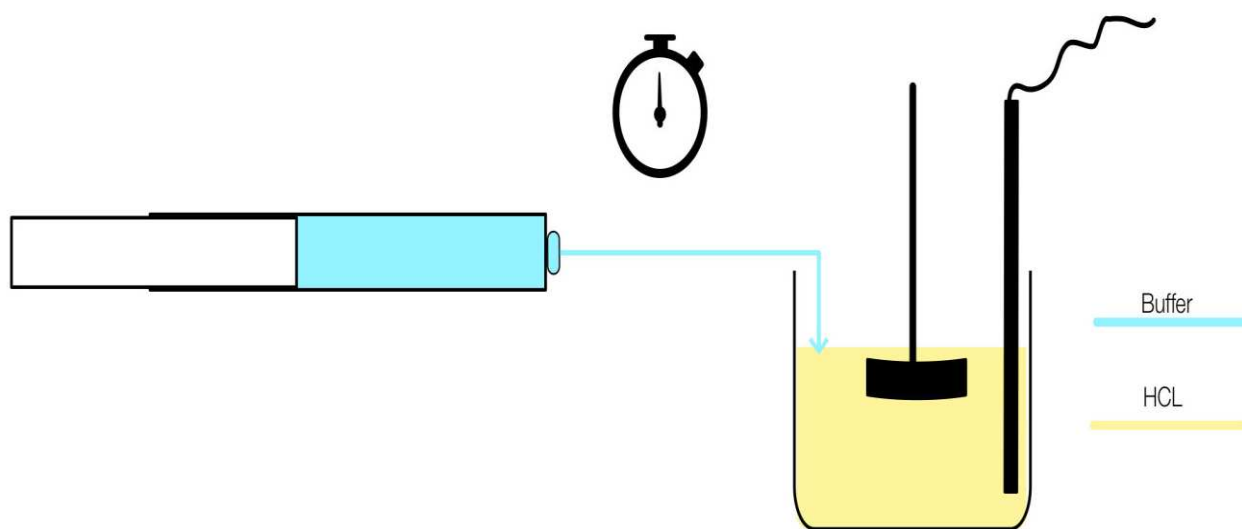


Figure 2.1: IDR experimental design while monitoring pH. The experimental

conditions (disk speed, flow rate, time) were adjusted to produce measurable concentrations and a linear relationship for each drug.

## **2.2. Biphasic Dissolution**

### **2.2.1. Analytical Method**

UV spectroscopy was used to measure the IBU in the buffer and octanol. A scan of IBU UV absorption was performed to determine the maximum wavelength absorption ( $\lambda_{\text{max}}$ ) in the buffer and in the octanol phase.

### **2.2.2. Franz Cell Biphasic Dissolution**

A 150 mL amount of 5 mM PBS was preheated in a jacketed vessel equipped with a three-paddle mixer, mixing at 100 rpm. The Franz cell donor chamber was closed, with two small tubes – one an inlet from the main vessel and the other an outlet back to the main vessel – and a hydrophilic membrane separating the donor and receptor chambers.

The Franz cell sampling port was closed to avoid a pressure difference (Figure 2.2). A tablet containing 600 mg IBU, 600 mg calcium sulfate, and 600 mg magnesium phosphate was tested in the main vessel for 60 min. Then, a 5 mL sample was taken from the main vessel and replaced with fresh medium, and a 0.5 mL sample was taken from Franz cell without replacement.

### **2.2.3. Laminar Flow Biphasic Dissolution**

Two jacketed vessels were preheated to  $37^{\circ}\text{C}\pm 0.5^{\circ}\text{C}$ . In one vessel (A), containing 150 mL of the buffer, a three-blade paddle was stirring at 100 rpm. The second vessel (B) was filled with 100 mL of the buffer and 50 mL of octanol, and two peristaltic pumps (Gilson Medical Electronics, France and Masterflex, Cole-Parmer, Chicago, USA) were used to circulate the buffer between Vessel A and Vessel B and back. A mixer was developed in-house, designed to produce close to laminar flow. This had four rounded rods attached to a cylindrical disk (Figure 2.3) and the stirrer speed was 75 rpm.

#### **2.2.3.1. Ibuprofen Partitioning**

A 50 mg sample of IBU was dissolved in 250 mL of 5 mM PBS. The solution was sonicated in an ultrasonic bath until a clear solution was obtained. Then the experimental setup described above (method in 2.2.3) was used, with the pump speed set at 5 mL/min. Then, a 1 mL sample was taken without replacement at 5, 10, 15, 20, 30, 45, 60, 75, 90, 120, 150, and 180 min.



### 2.2.3.2. Ibuprofen Biphasic Dissolution

The buffer (either 5 mM PBS or 10 mM bicarbonate) was preheated to  $37^{\circ}\text{C}\pm 0.5^{\circ}\text{C}$ , then 30 mg of IBU was placed in Vessel A, for 90 min at 10 mL/min. A 5 mL buffer sample was taken with medium replacement, and a 1 mL octanol sample without replacement.  $\text{CO}_{2(\text{g})}$  was supplied above Vessel A when BCB was used, while the pH was monitored to emulate the 5 mM PBS pH. The BCB concentration was verified using a Thermo Scientific Orion Carbon Dioxide Electrode.

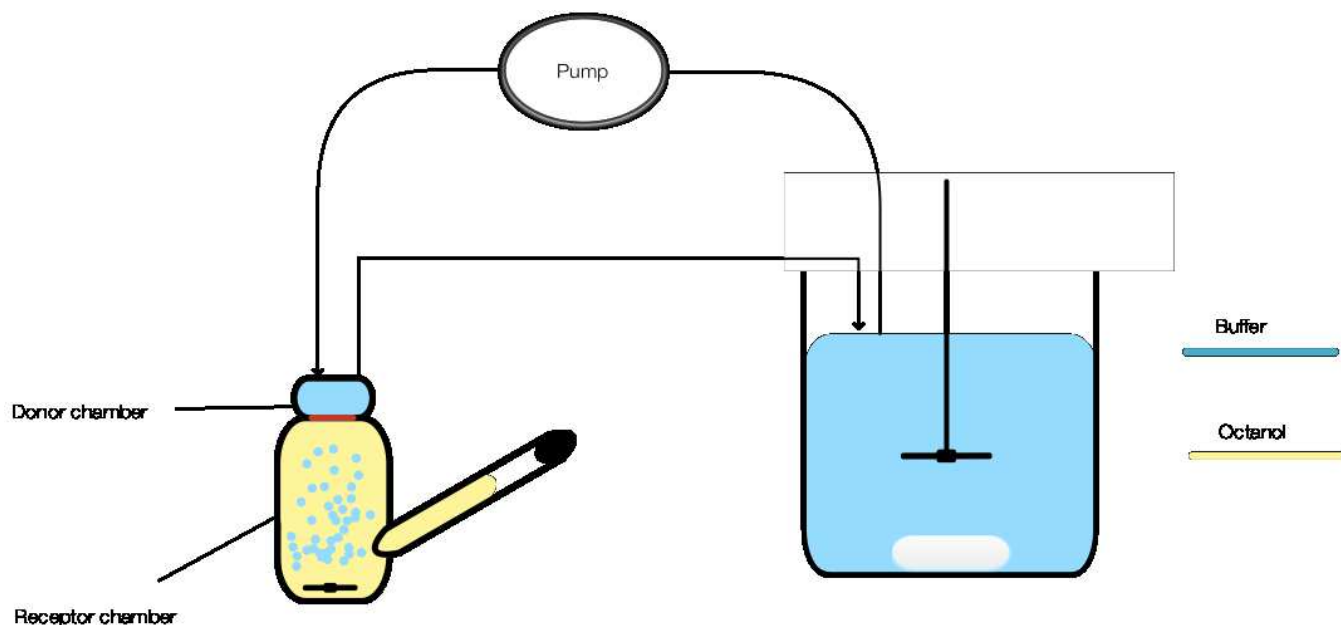


Figure 2.2: Illustration of biphasic dissolution using of Franz cells. Octanol phase (yellow) in Franz cells, buffer (blue) in main vessel, with IBU (white), being stirred

at 100 rpm, with the media circulated at 5 mL/min. A hydrophilic membrane filter (red) was used

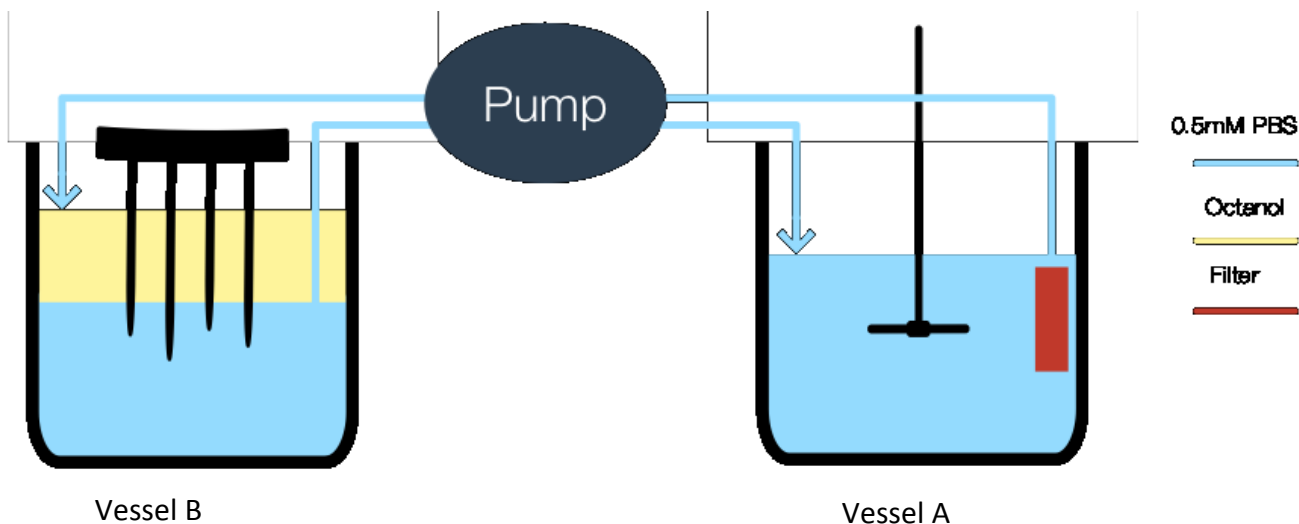


Figure 2.3: Illustration of the biphasic dissolution setup with the use of a stirrer. Octanol phase yellow, buffer blue in Vessel B. The medium was pumped at 10 mL/min between Vessels A and B.

### 2.3. Statistical Analysis

The data is presented as mean  $\pm$  standard deviation (SD). An unpaired student's two-tailed t-test (SPSS, Statistics Grad Pack) was used to test for statistical significance (p), the difference being considered statistically significant when  $p < 0.05$  at  $\alpha = 0.05$ . DDSolver was used for the multivariate model independent procedure (MMIP), and a similarity factor ( $f_2$ ) was used to compare dissolution profiles.<sup>47-50</sup>

# **Chapter Three**

## **Result**

### 3. Result:

#### 3.1. High Pressure Liquid Chromatography Assay:

Plotting AUC against concentration showed a linear relation for IBU and GRI. IBU and GRI are stable in the media and mobile phase used in preparing the stander curve, as shown by other studies, therefore, less than 6 data points were used to make the stander curve. Both HPLC methods for IBU and GRI were adapted with minor changes from published studies, so an in-house validation was not nessesary.<sup>51</sup> The calibration curves are shown in Figure 3.1 and Figure 3.2.

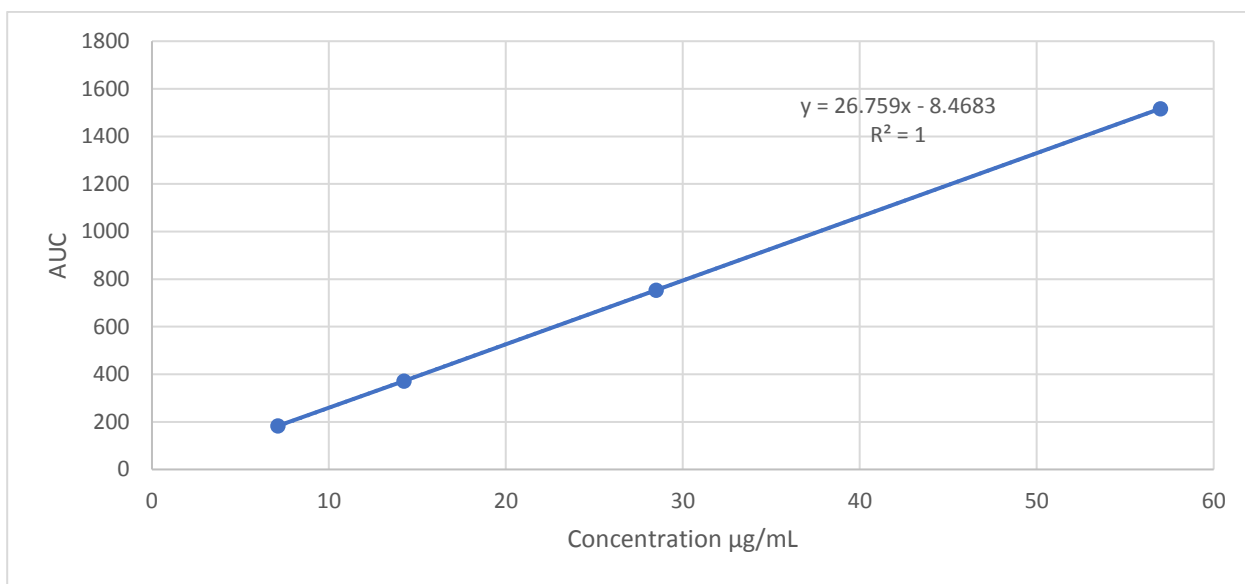


Figure 3.1: Standard curve for IBU. The error bars represent the mean  $\pm$  upper and lower limits (n=2).

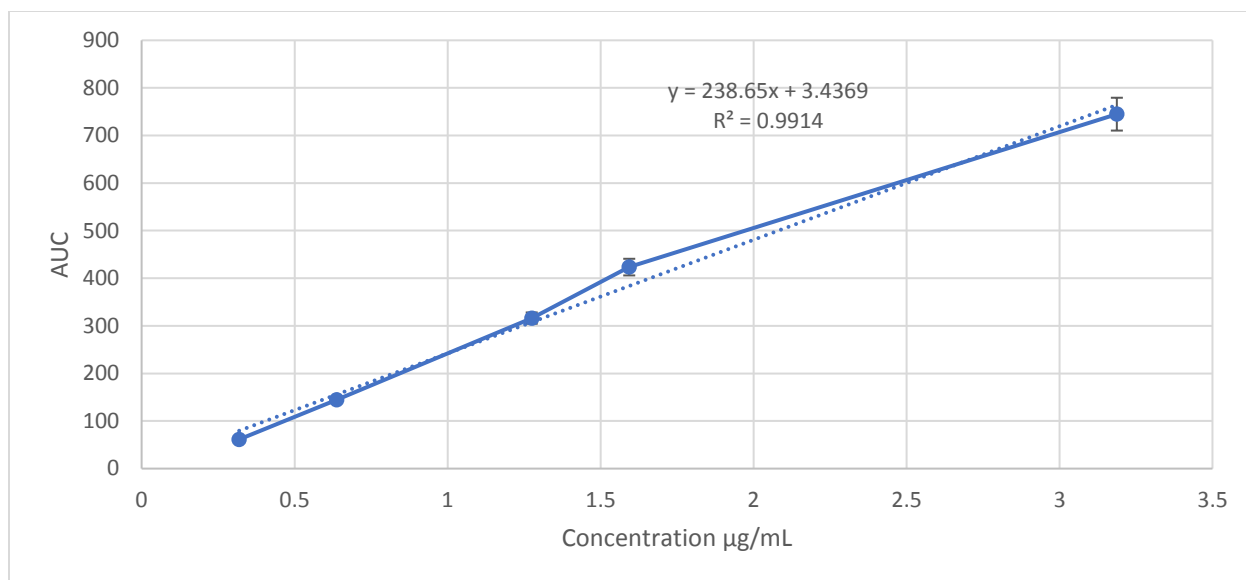


Figure 3.2: Standard curve for GRI. The error bars represent the upper and lower limits (n=2).

### 3.2. Ibuprofen Intrinsic Dissolution Rate

The experiments were performed in order to study the effect of buffer strength, buffer composition, and surfactant on low-solubility acidic drugs.

#### 3.2.1. Using 50 mM Phosphate Buffer

Figure 3.3 shows the concentration over time relationship, which is linear, with a coefficient of determination ( $R^2$ ) of 0.9895.<sup>52</sup> The concentration was 0.21 for the first time point, and almost 10 times that at the end of the experiment, where the slope was 0.114, giving an IDR of  $0.228 \text{ mg/min.cm}^2 \pm 0.018$ , as shown in Figure

3.4. The pH started at 2.9 at the first time point, increased to 6.6 at 3 min, and then maintained stability until the end of the experiment (Figure 3.5).

### **3.2.2. Using 10 mM Phosphate Buffer**

A linear relationship between time and concentration was found, with  $R^2=0.9835$  (Figure 3.3). The concentration maintained a steady increase over the 20 min of the test, with a slope of 0.0452. Using Eq. 1.1, IBU produced an IDR of  $0.090 \text{ mg/min.cm}^2 \pm 0.003$  (Figure 3.4). The difference from the 50 mM PBS was significant, with  $p<0.001$  (Table 3.1). The medium pH started at pH 2.8, reaching over pH 6.0 after 4 min; the pH remained constant at pH 6.6 after 9 min (Figure 3.5).

### **3.2.3. Using 10 mM Bicarbonate Buffer**

The IBU intrinsic dissolution in the BCB showed a similar linear characteristic, with  $R^2=0.9953$ , the slope being 0.034 (Figure 3.3). The IDR (Figure 3.4) was  $0.068 \text{ mg/min.cm}^2 \pm 0.003$ . The difference between the BCB and the 10 and 50 mM PBS was significant, with  $p=0.001$  and  $p<0.001$ , respectively (Table 3.1). The pH started at pH 2.8, increasing to  $>6.0$  after 6 min. Then, a steady pH of 6.6 was achieved after 13 min (Figure 3.5).

### **3.2.4. Using 50 mM Phosphate Buffer with Bile Salts**

The 50 mM phosphate buffer with bile salts (PBBS) gave a linear curve (Figure 3.6), with  $R^2=0.9869$  and a slope of 0.1179. The IDR was  $0.213 \text{ mg/min.cm}^2 \pm 0.004$  (Figure 3.4), and there was no significant difference this between 50mM PBS ( $p=0.272$ ). PBBS produced a similar pH profile to 50 mM PBS (Figure 3.7).

### **3.2.5. Using 10 mM Phosphate Buffer with Bile Salts**

The 10 mM PBBS showed linear relationship between time and concentration, with  $R^2=0.9909$ . The slope of the curve was 0.0464 (Figure 3.6) and the IDR  $0.093 \text{ mg/min.cm}^2 \pm 0.007$  (Figure 3.4). There was no significant difference between 10 mM PBBS and 10 mM PBS ( $p=0.541$ ), however there was a difference when compared to 50 mM PBBS ( $p<0.001$ ; Table 3.1). The pH of the medium over time (Figure 3.7) showed a huge increase between 3 and 6 min, after which the pH remained steady until the end of the experiment, reaching pH 6.6.

### **3.2.6. Using 10 mM Bicarbonate Buffer with Bile Salts**

The BBBS gave a linear relation, with  $R^2=0.993$  and a slope of 0.0369 (Figure 3.6), giving  $0.074 \text{ mg/min.cm}^2 \pm 0.003$  (Figure 3.4). There was a significant difference between 10 mM BBBS, 10 mM PBBS, and 50 mM PBBS, with  $p=0.01$  and  $p<0.001$ , respectively, but no significant difference compared to BCB

( $p=0.082$ ), as shown in Table 3.1. The BBBS pH profile showed a similar pattern to that of BCB (Figure 3.7).

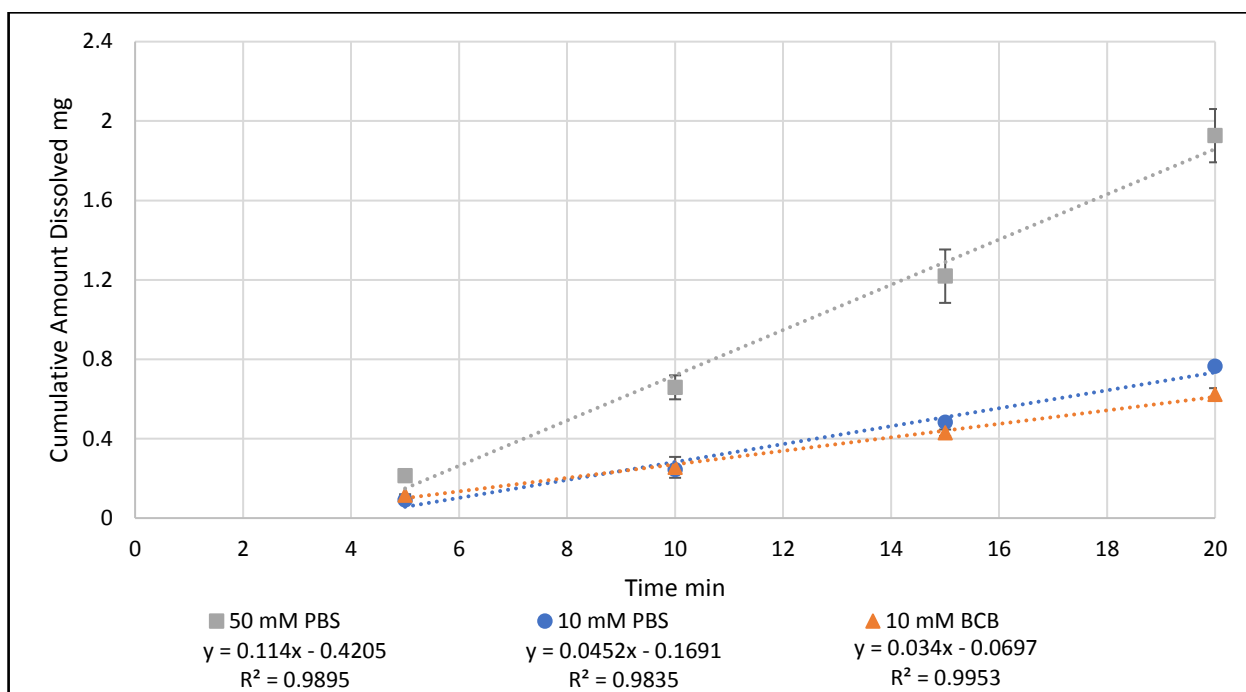


Figure 3.3: The effects of buffer strength and composition on the cumulative amount of dissolved of IBU (mg) at a speed of 100 rpm, and at 37°C, the disk was compressed at a force of 1,000 psi. The linear trend estimation is shown as a dotted line. The error bars represent the mean  $\pm$  SD (n=3).



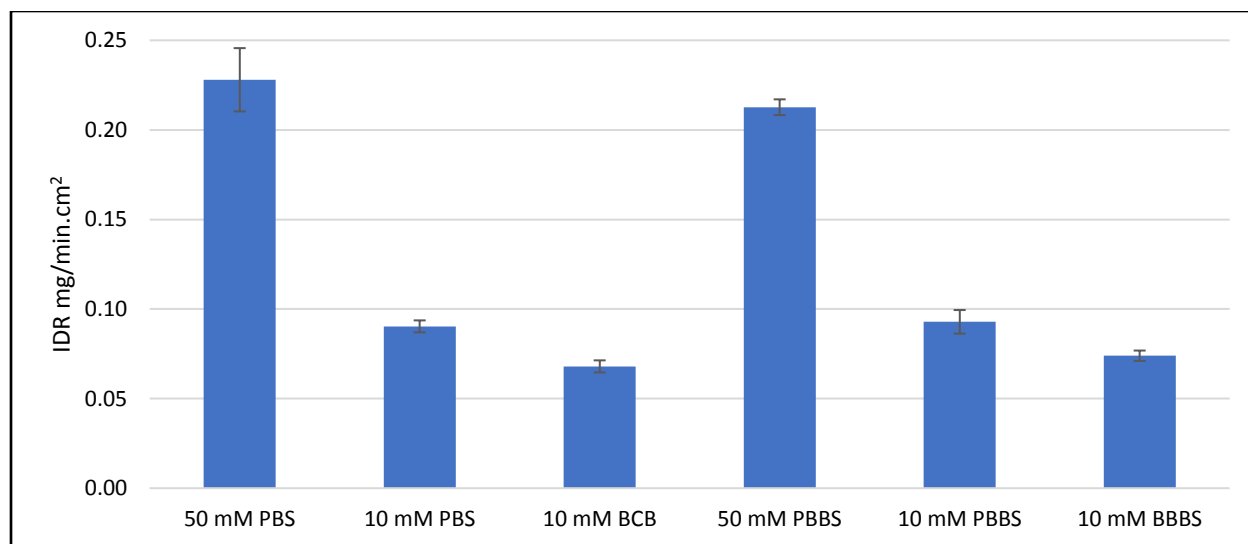


Figure 3.4: The effects of buffer strength, composition, and surfactant on the IBU IDR in mg/min.cm<sup>2</sup>. The IDR was calculated by dividing the slope by the disk area (0.5 cm<sup>2</sup>). The error bars represent the mean  $\pm$  SD (n=3).

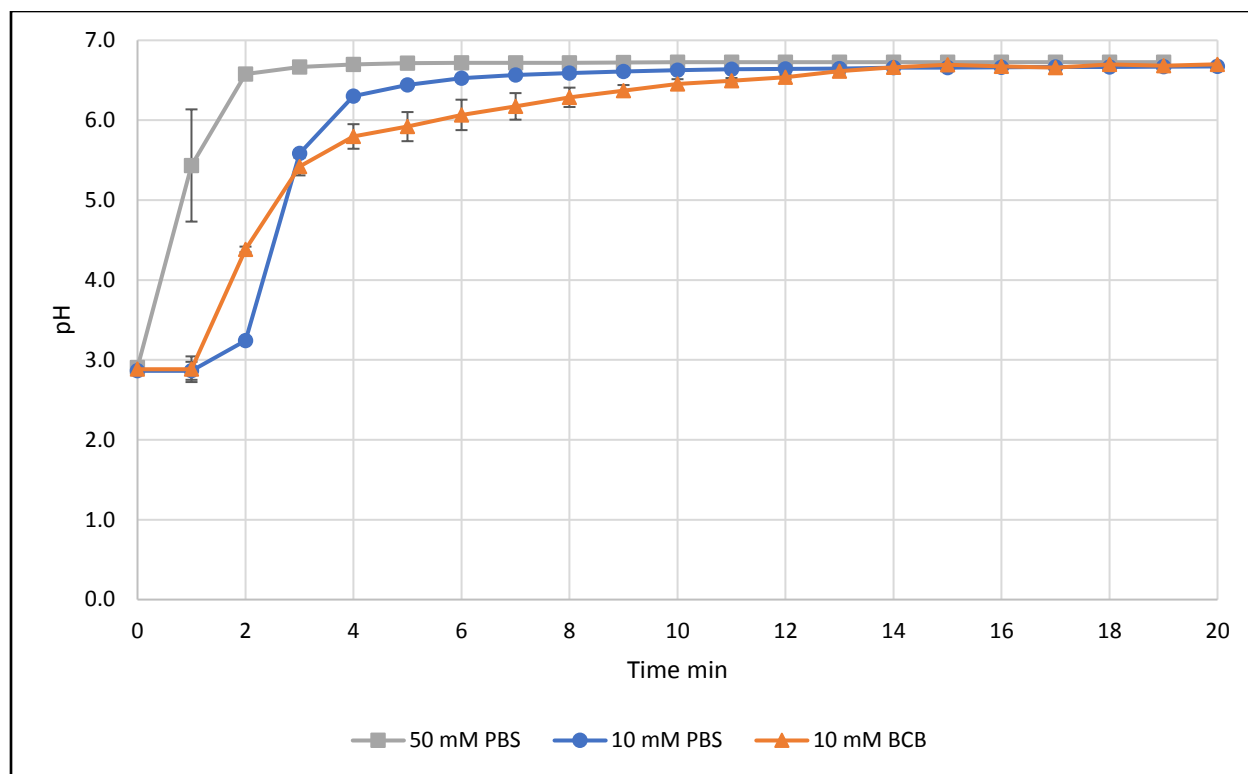


Figure 3.5: The effect of buffer strength and composition on pH in the presence of IBU. The error bars represent the mean  $\pm$  SD (n=3).

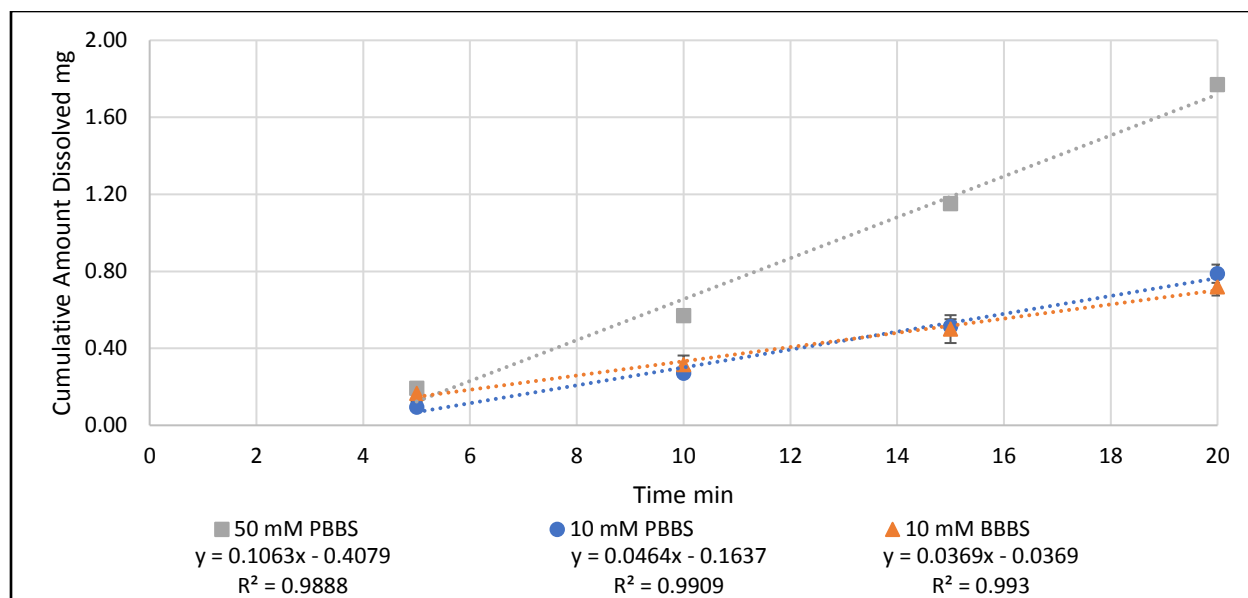


Figure 3.6: The effect of buffer strength, composition, and surfactant on the cumulative amount of IBU dissolved (mg). at a speed of 100 rpm, and 37°C, where the disk was compressed with a force of 1000 psi. The linear trend estimation is shown as a dotted line. The error bars represent the mean  $\pm$  SD (n=3).

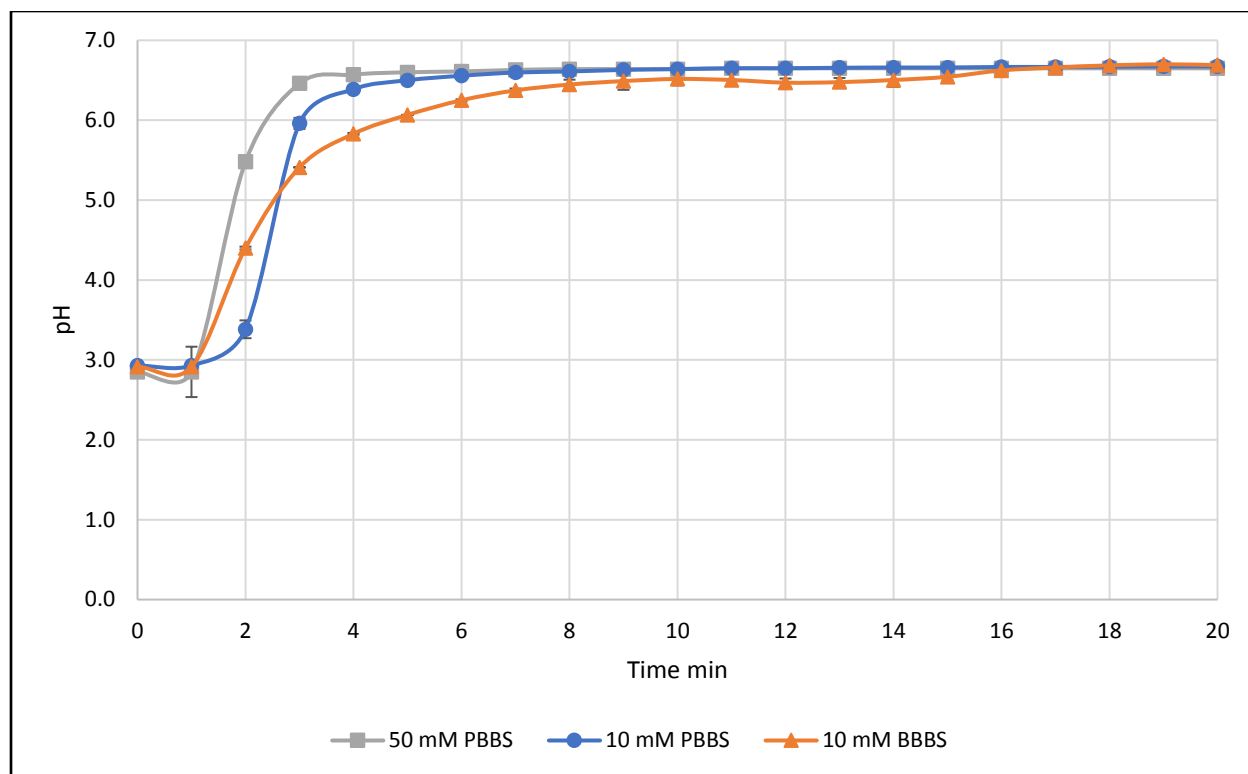


Figure 3.7: The effect of buffer strength, composition, and surfactant on pH. The error bar represent the mean  $\pm$  SD (n=3).

<b>Media A</b>	<b>Media B</b>	<b>p value</b>
50 mM PBS	10 mM PBS	<0.001*
10 mM BCB	50 mM PBS	<0.001*
10 mM PBS	10mM BCB	0.001*
50 mM PBBS	10 mM PBBS	<0.001*
10 mM PBBS	10 mM BBBS	0.01*
10mM BBBS	50 mM PBBS	<0.001*
50 mM PBS	50 mM PBBS	0.272
10 mM PBS	10 mM PBBS	0.541
10 mM BCB	10 mM BBBS	0.082

Table 3.1: P values for the IBU IDR in different media, using the two-tailed t test;

\*indicates a significant difference.

### **3.3. Griseofulvin IDR**

Experiments were performed in order to study the effects of buffer composition and surfactants on a low-solubility neutral drug.

#### **3.3.1. Using 10 mM Phosphate Buffer**

The GRI intrinsic dissolution in PBS was  $R^2=0.995$ , indicating a linear relation between concentration and time (Figure 3.8), and a 0.0004 slope. The PBS gave an IDR of  $0.867 \mu\text{g}/\text{min}\cdot\text{cm}^2 \pm 0.115$  (Figure 3.9). The pH showed a slow increase in the first 20 min, to approach pH 6.0, and reached pH 6.5 after 1 hr (Figure 3.10).

#### **3.3.2. Using 10 mM Bicarbonate Buffer**

The BCB produced similar curves to the PBS for the first two data points, but showed a minor increase in concentration for the last two data points (Figure 3.8). The  $R^2=0.995$ , and the slope was 0.0005, resulting in a slightly higher IDR ( $1.066 \mu\text{g}/\text{min}\cdot\text{cm}^2 \pm 0.115$ ) than for the PBS (Figure 3.9). The difference between the GRI IDR of the PBS and BCB was not significant ( $p=0.101$ ; Table 3.2). The pH reached pH 5.0 in the first 10 min, then continued to increase until it reached pH 6.5 after 30 min, and stayed around that pH until the end of the experiment (Figure 3.10).

### **3.3.3. Using 10 mM Phosphate Buffer with Bile Salts**

The PBBS medium produced a linear curve throughout the experiment (Figure 3.11), with  $R^2=0.987$ , and a slope of 0.0006, giving an IDR of  $1.2 \mu\text{g}/\text{min}\cdot\text{cm}^2$  (Figure 3.9). The difference between the PBBS and PBS was significant, with  $p=0.007$  (Table 3.2). The pH of the PBBS showed a similar pattern to that of the PBS pH profile (Figure 3.12). The average micelle diameter size was  $160 \text{ nm} \pm 30.5$  (Figure 3.11).

### **3.3.4. Using 10 mM Bicarbonate Buffer with Bile Salts**

GRI produced a linear relation, with  $R^2=1$  (Figure 3.11), while the slope was 0.0011. The IDR was  $2.2 \mu\text{g}/\text{min}\cdot\text{cm}^2 \pm 0.0022$  (Figure 3.9), which is significantly higher compared to the PBBS and BCB, with  $p<0.001$  in both cases (Table 3.2). The pH curve of the BBBS (Figure 3.12) increased dramatically in the first 5 min, reaching pH 5.0, and continued to increase, reaching pH 6.5 after 1 hr. The average micelle diameter size was  $274.4 \text{ nm} \pm 5.9$ .

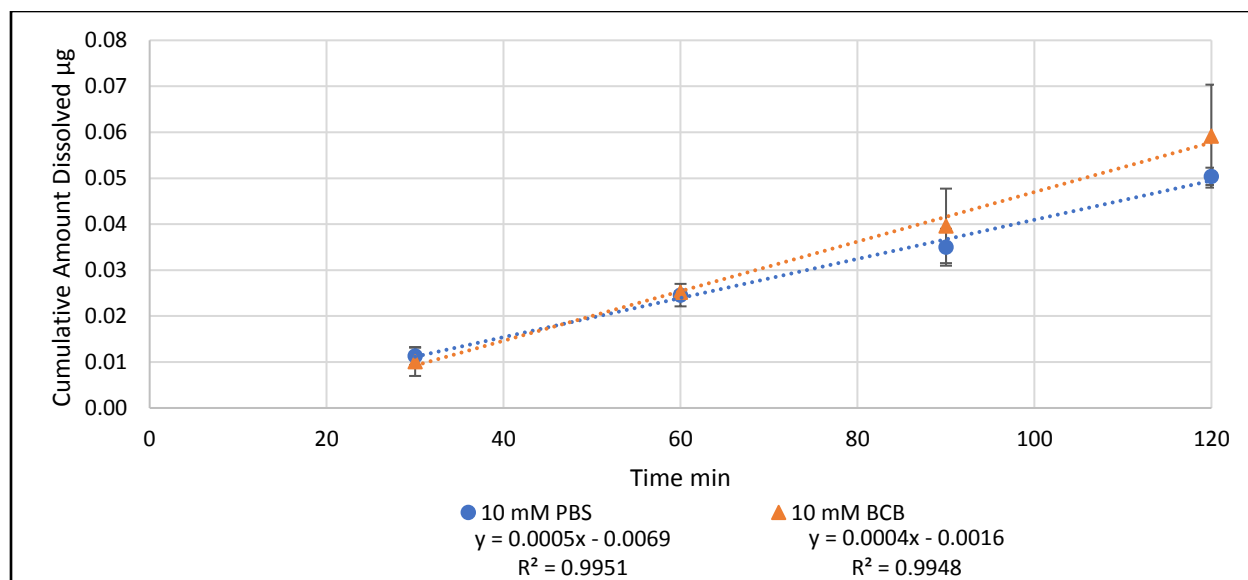


Figure 3.8: The effects of buffer composition and surfactant on cumulative GRI dissolved ( $\mu\text{g}$ ). at a speed of 200 rpm, and  $37^\circ\text{C}$ , the disk was compressed at a force of 4000 psi, The linear trend estimation is shown as a dotted line. The error bars represent the mean  $\pm$  SD (n=3).



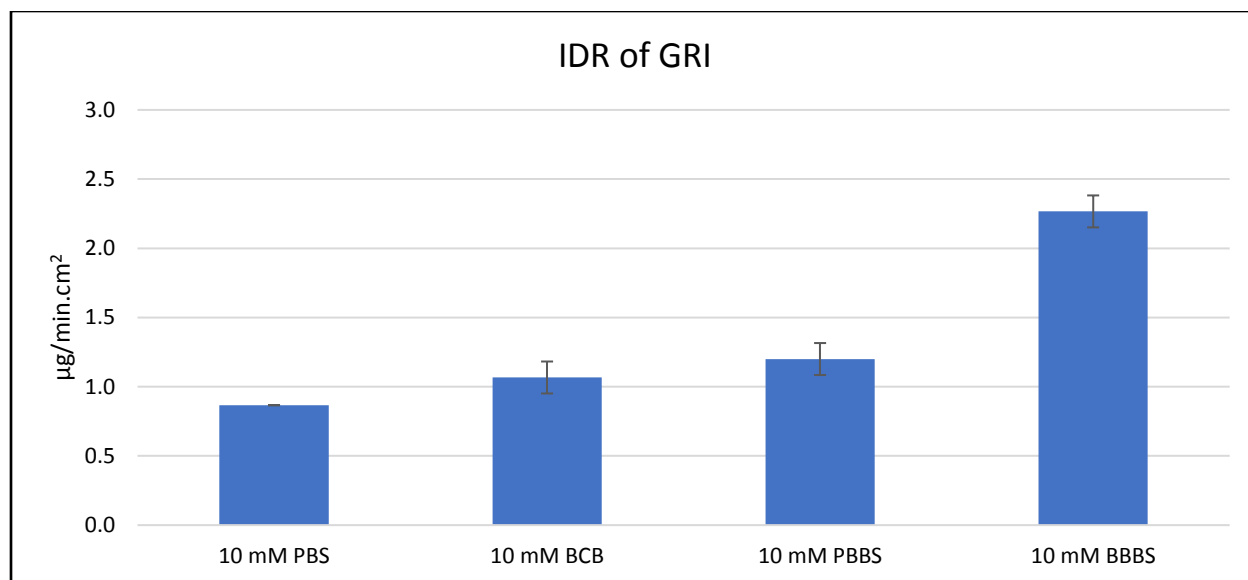


Figure 3.9: The effects of buffer composition and surfactant on the GRI IDR in  $\mu\text{g}/\text{min}\cdot\text{cm}^2$ . The IDR was calculated by dividing the slope by the disk area ( $0.5\text{ cm}^2$ ). The error bars represent the mean  $\pm$  SD ( $n=3$ ).

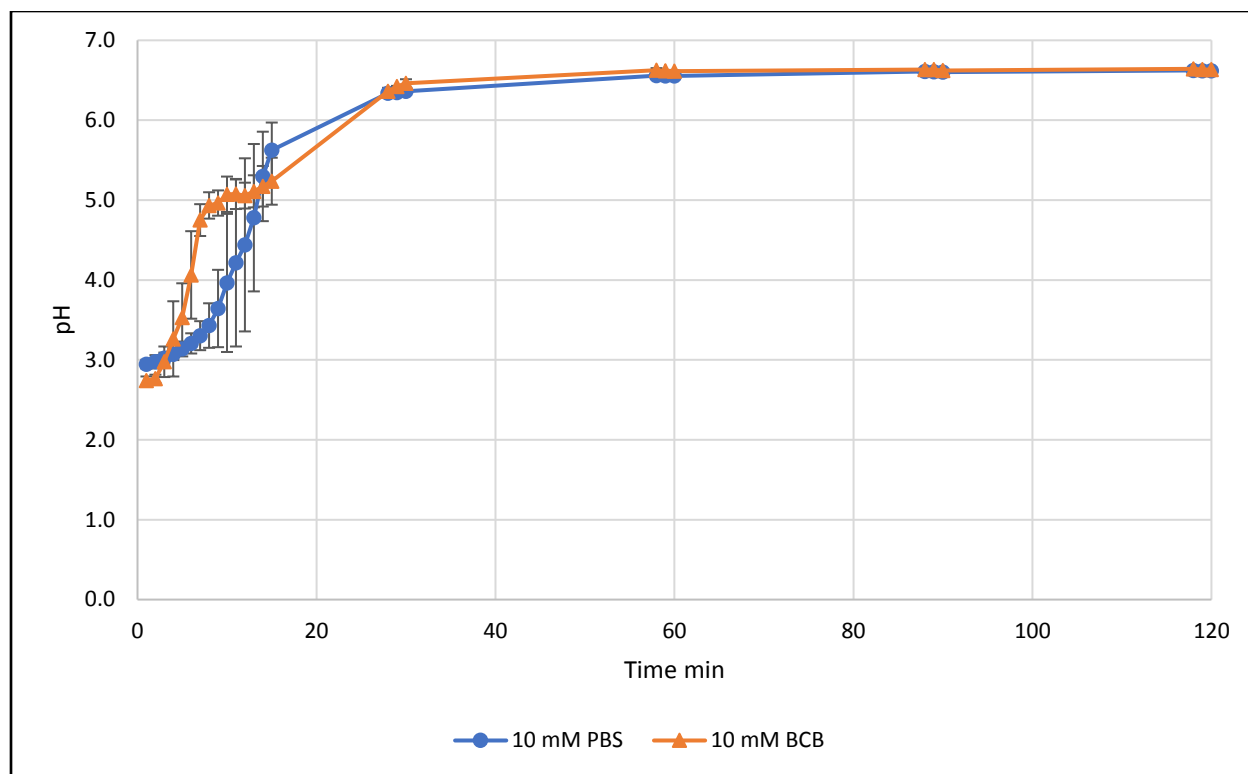


Figure 3.10: The effect of buffer composition on pH. The error bar represent the mean  $\pm$  SD (n=3).

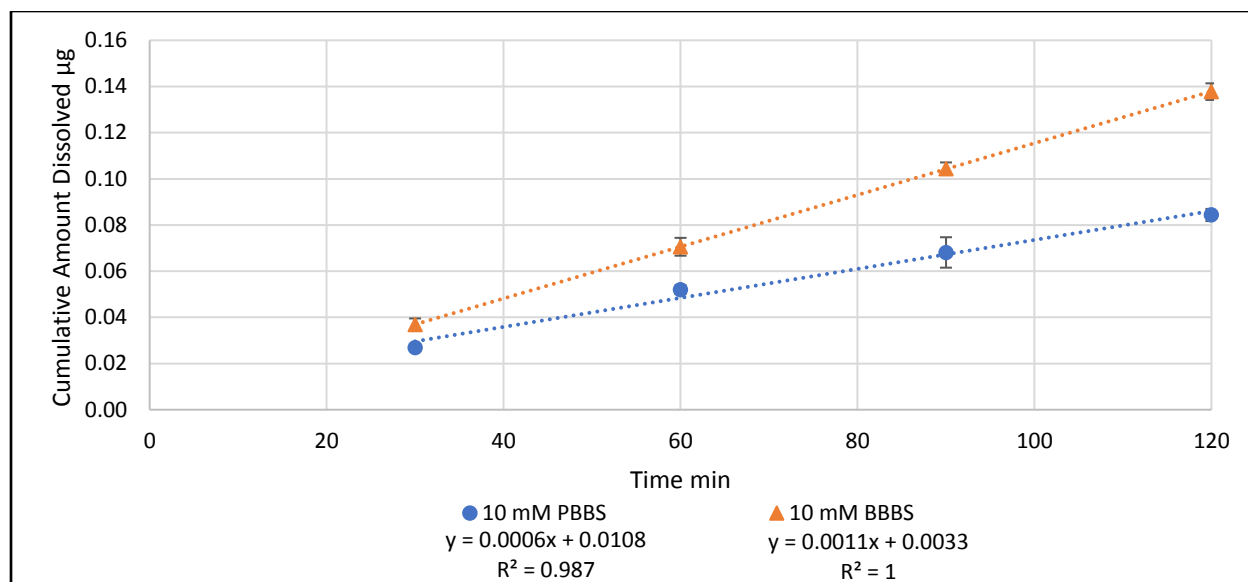


Figure 3.11: The effect of buffer composition on cumulative dissolved GRI ( $\mu\text{g}$ ). at speed of 200 rpm, and  $37^\circ\text{C}$ , where the disk was compressed at force of 4000 psi, The linear trend estimation is shown as a dotted line. The error bars represent the mean  $\pm$  SD (n=3).

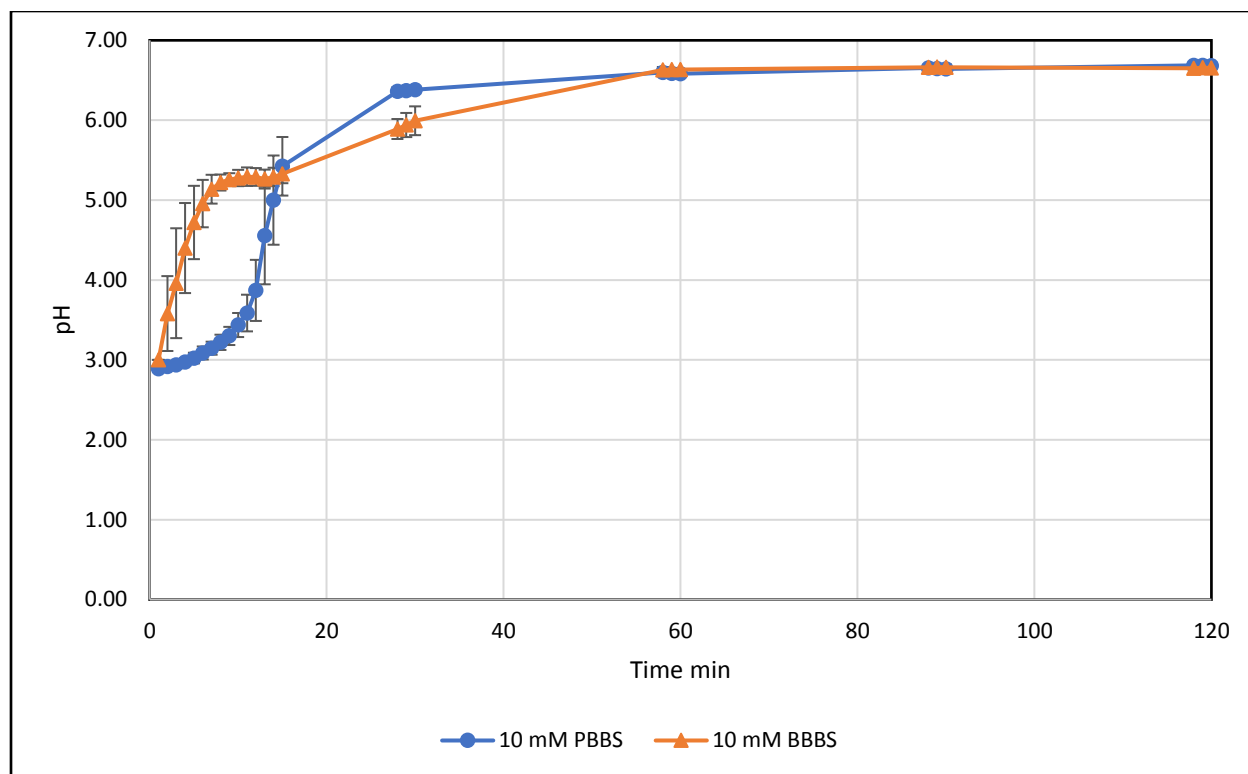


Figure 3.12: The effect of buffer composition on pH. The error bar represent the mean  $\pm$  SD (n=3).

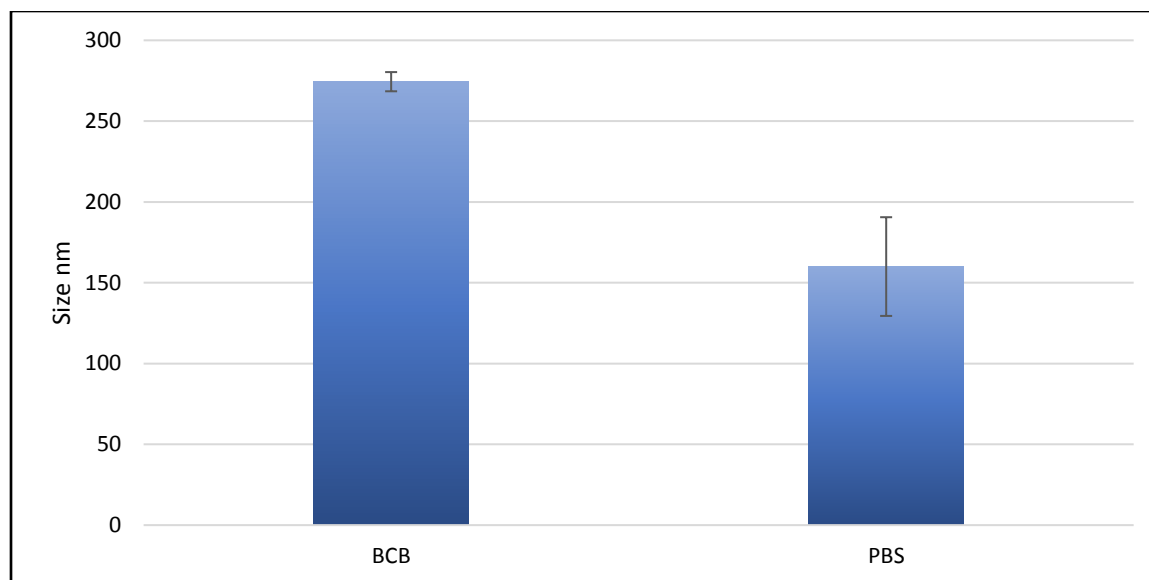


Figure 3.13: Average diameter (nm) of bile salts micelles in 10 mM BCB and 10 mM PBS. The error bars represent the upper and lower limits (n=2).

Media A	Media B	p value
PBS	BCB	0.101
PBBS	BBBS	<0.001*
PBS	PBBS	0.007*
BCB	BBBS	<0.001*

Table 3.2: P values for the GRI IDR in different media, using the two-tailed t test.

\*Indicates a significant difference.

### **3.4. Two-Compartment Biphasic Dissolution Results**

The aim of these experiments was to develop a biphasic dissolution system that allowed for effective CO<sub>2(g)</sub> addition without interfering with the hydrodynamics in the dissolution vessel.

#### **3.4.1. IBU UV Scan:**

The  $\lambda_{\max}$  found to be 221 nm in the buffer, and 260 nm in the octanol. Those wave lengths were used to analyze the samples. Octanol caused redshift in IBU as a result of solvatochromism.<sup>53</sup>

#### **3.4.2. Franz Cell IBU Biphasic Dissolution System**

The Franz cell biphasic dissolution experiment (Figure 3.14) took an hour. The maximum concentration of IBU was 68.69 mg/mL in 5 mM PBS, and 0.724 mg/mL in the octanol phase, by the end of the experiment, when the total cumulative dissolution was 13.03%; however, the stability of the system was a major problem, as the octanol sample was contaminated with a small volume of the buffer. Also, with time, the octanol appeared to have escaped from the Franz cell and reached the main dissolution vessel.

The pH showed an interesting pattern. The medium maintained the pH at >6.35 for the first 10 min, when the concentration of IBU was about 30 mg/mL, as shown

in Figure 3.15. Then, the pH declined as the IBU concentration increased, until the end of the experiment, at which point the pH was 5.87.

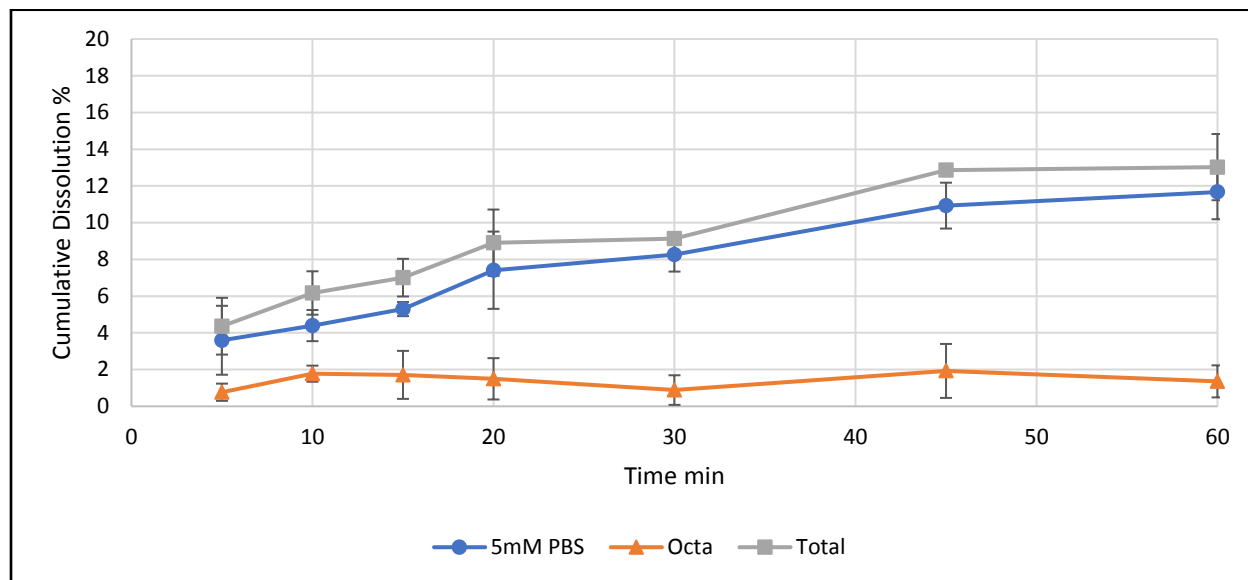


Figure 3.14: Cumulative % dissolution of IBU using a mixer, with 200  $\mu\text{g}/\text{mL}$  IBU (250 mL 5 mM PBS), 50 mL octanol (Octa), and the total percentage dissolved (paddle speed 100 rpm, laminar mixer speed 75 rpm, at 37°C). The error bars represent the upper and lower limits (n=2).

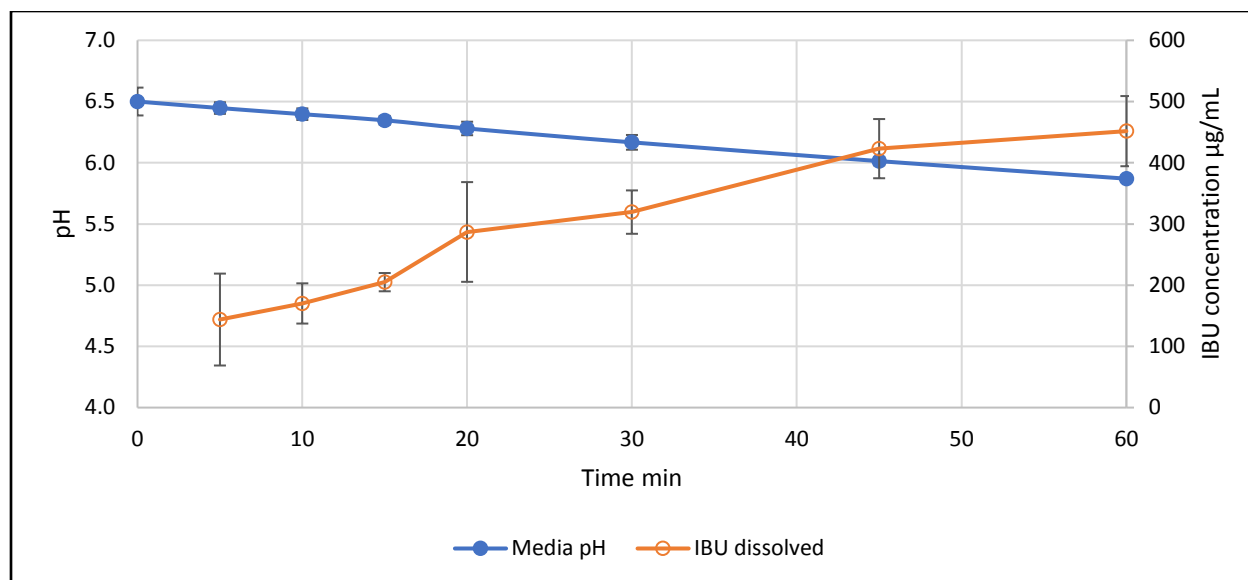


Figure 3.15: IBU dissolution medium pH (primary y axis), and concentration of IBU dissolved mg/mL (secondary axis), using Franz cells. The error bars represent the mean  $\pm$  SD (n=3).

### 3.4.3. Ibuprofen Biphasic Dissolution Using Laminar Flow Mixer

#### 3.4.3.1. Partitioning of Ibuprofen

The IBU dissolved in the buffer (Figure 3.16) was 103.9% after 5 min, and the total dissolved was 118.12%. The total dissolved remained above 100% for 45 min, then came down below 100% until the end of the experiment.

The buffer IBU dissolved steadily decreased to 11.84% after 180 min, while the IBU dissolved in octanol increased to 85.7%. The pH was 5.9 at the beginning of the experiment. With the partitioning of IBU into the octanol phase, the pH increased to pH 6.47 after 180 min (Figure 3.17).



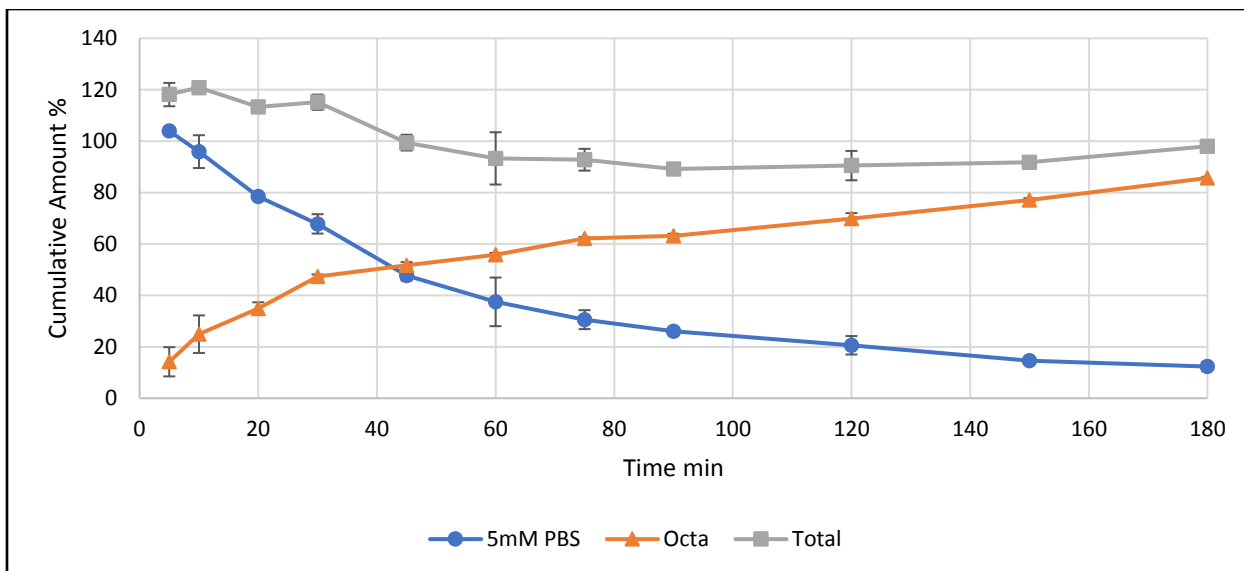


Figure 3.16: Cumulative % dissolution of IBU using a mixer; 200  $\mu\text{g}/\text{mL}$  IBU (250 mL 5 mM PBS), 50 mL octanol (Octa), and total percent dissolved (paddle speed 100 rpm, laminar mixer speed 75 rpm, at 37°C). The error bars represent the upper and lower limits (n=2).

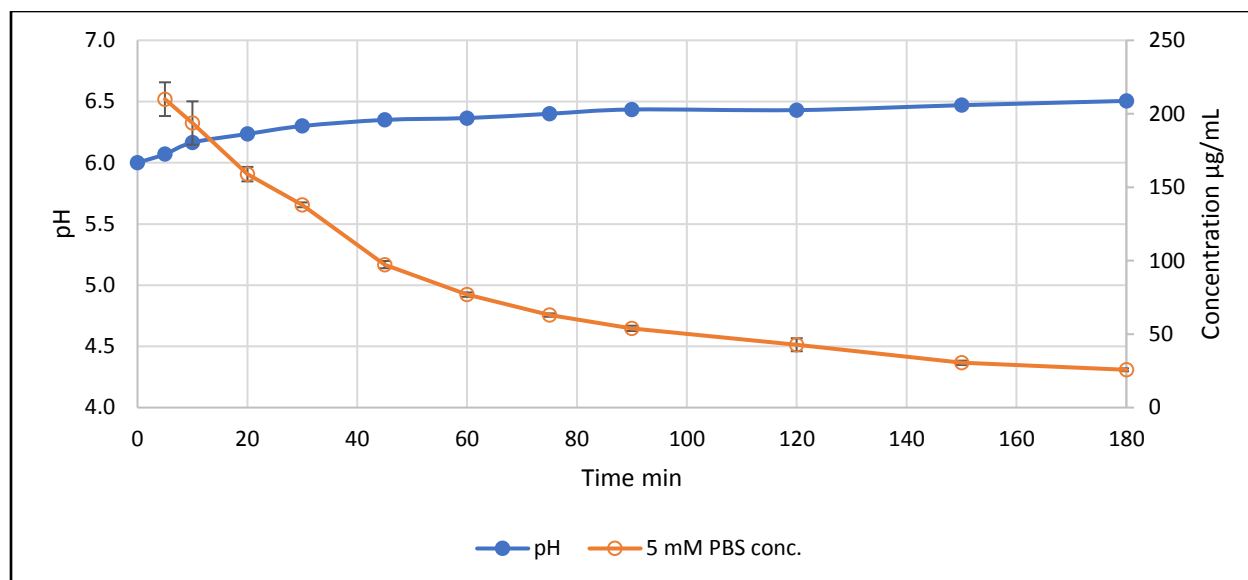


Figure 3.17: IBU buffer dissolution medium pH (primary y axis) and concentration of IBU mg/mL (secondary axis) over time, using a mixer. The error bars represent the mean  $\pm$  upper and lower limits (n=2).

### 3.4.3.2. Ibuprofen Biphasic Dissolution

#### 3.4.3.2.1. Biphasic Dissolution in 5 mM Phosphate Buffer

Dissolution in the 5 mM PBS phase (Figure 3.18) continued to increase to a maximum of around 70% (21.5 mg) at 20 min, then the IBU was partitioned into the octanol phase, which produced a zero order pattern, with the zero order dissolution constant  $k_0=0.626 \pm 0.055$ , where the octanol flux was  $0.132 \mu\text{g}/\text{min}\cdot\text{cm}^2 \pm 0.009$ . At the end, 26.6% of the dissolved IBU was in the buffer, whilst 55.4% was in the octanol phase. The total amount remained the same at around 92% after 45 min. The pH of the buffer reached a minimum of 6.4 at 20 min (Figure 3.19), at the same time

as the highest concentration ( $C_{\max}$ ). The pH then continued to increase as the IBU moved into the octanol phase, ending at pH 6.47.

#### **3.4.3.2.2. Dissolution in 10 mM Bicarbonate Buffer**

The BCB dissolution curve (Figure 3.20) showed an increase in the amount of IBU dissolved up to a maximum of 18.9 mg at 30 min, while it steadily increased in the octanol phase up to the end of the experiment, with 38% IBU in that. The zero order dissolution constant was  $0.431 \pm 0.116$ , while the octanol flux was  $0.087 \mu\text{g}/\text{min}\cdot\text{cm}^2 \pm 0.024$ . The total amount of IBU in the two phases reached a maximum at the end of the experiment, with 88.4% dissolved. The pH of the BCB was constant over the experiment duration, with a lower limit at pH 6.47 at 30 min, and  $\text{pH } 6.5 \pm 0.03$  at the end, as shown in Figure 3.21.

#### **3.4.3.2.3. Biphasic Dissolution Profile Comparison**

The similarity between the 5 mM PBS and 10 mM BCB phases was not statistically significant for any time points, using the MMIP, as shown in Table 3.3. There were similarities for the first four time points in the octanol phase, but the last three time points were not similar. The total IBU dissolved showed a similarity only at 30 min and 90 min; however, comparing the release pattern using  $f_2$  showed similarity at the edge (51%). The t test (Table 3.4) showed similar results to those

from the MMIP; however, some points showed significant differences ( $p < 0.05$ ), although the similarity assumption was accepted using the MMIP.

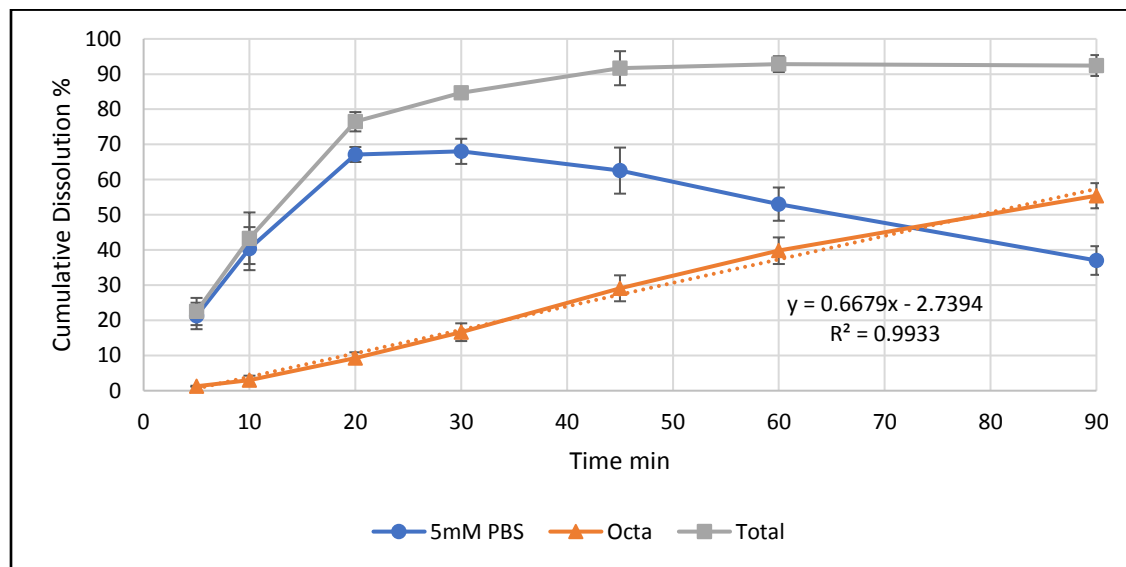


Figure 3.18: Cumulative % dissolution in 5 mM PBS using a mixer; 250 mL of 5 mM PBS, 50 mL of octanol (Octa), and total percent dissolved (paddle speed 100 rpm, mixer speed 75 rpm, at 37°C). The error bars represent the mean  $\pm$  SD (n=3).

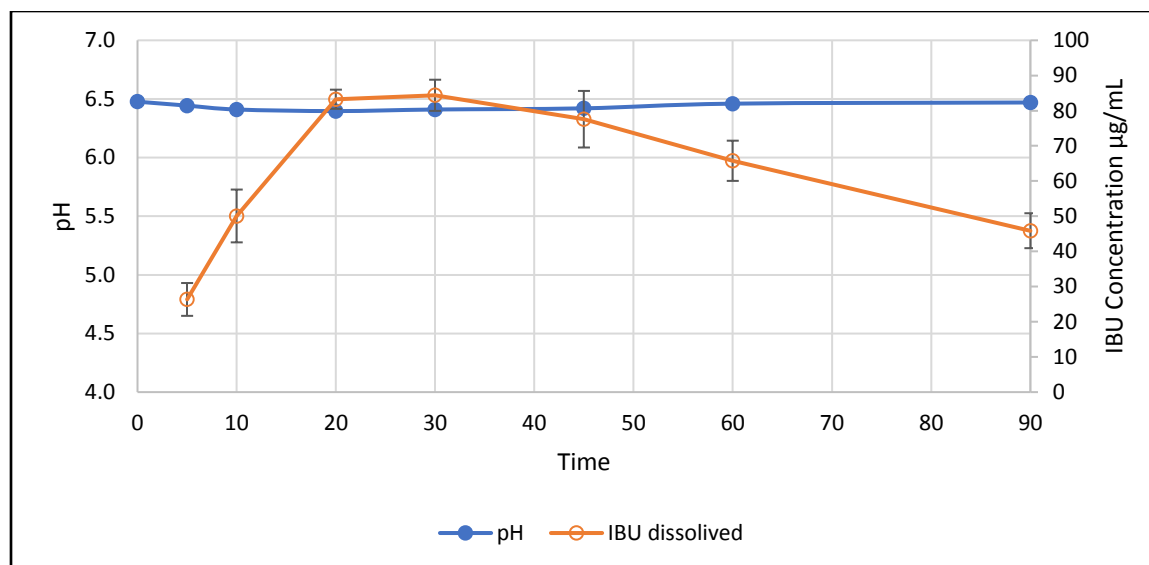


Figure 3.19: PBS medium pH (primary y axis) and concentration of IBU mg/mL (secondary axis) over time, using a mixer. The error bars represent the mean  $\pm$  SD (n=3).

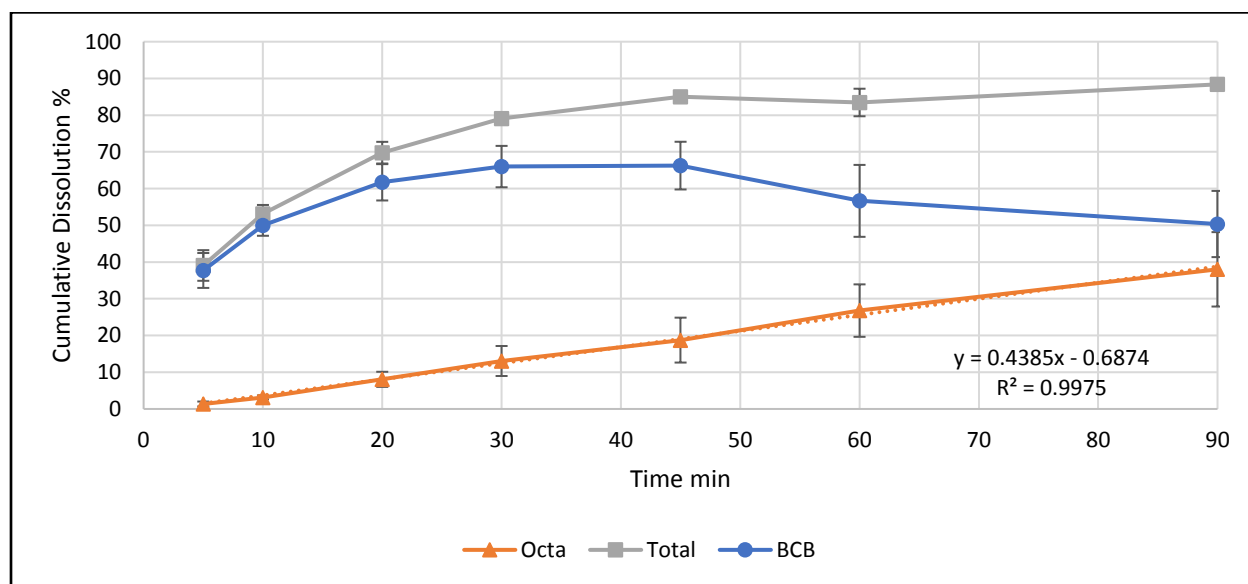


Figure 3.20: IBU biphasic cumulative dissolution percentage in 10 mM BCB using a mixer; 250 mL of 10 mM BCB, 50 mL octanol (Octa), and total percent dissolved

(100 rpm, mixer speed 75 rpm, at 37°C). The error bars represent the mean  $\pm$  SD (n=3).

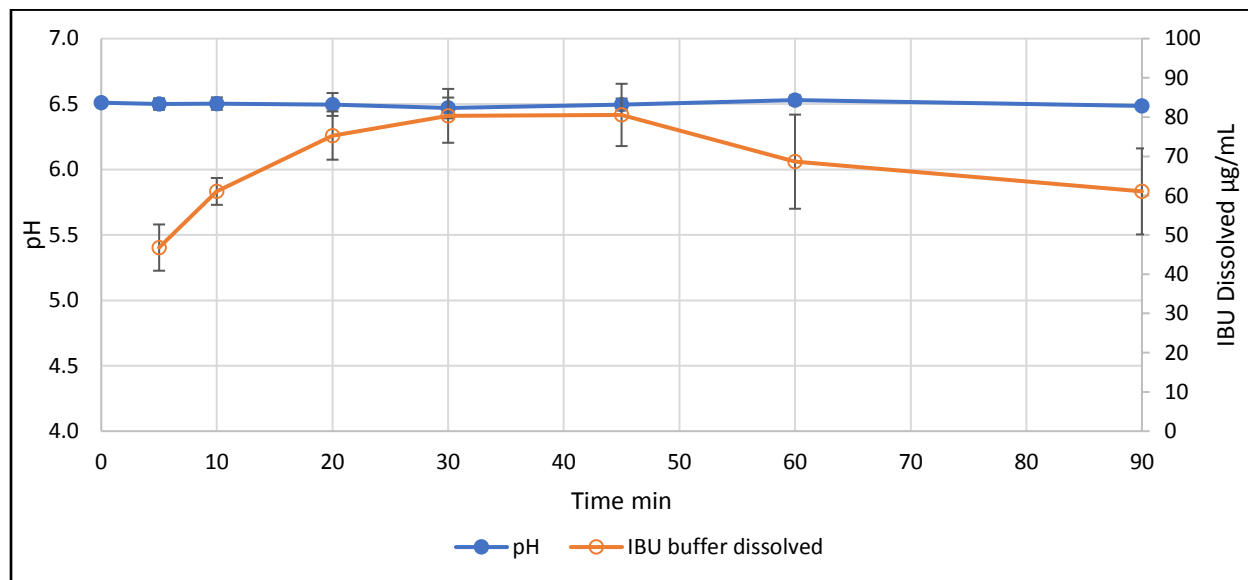


Figure 3.21: BCB medium pH (primary y axis) and concentration of IBU mg/mL (secondary axis) over time, using a mixer. The error bars represent the mean  $\pm$  SD (n=3).

<b>T test</b>	<b>Octa</b>	<b>Buffer</b>	<b>Total</b>
<b>5</b>	A	R	R
<b>10</b>	A	R	R
<b>20</b>	A	R	R
<b>30</b>	A	R	A
<b>45</b>	R	R	R
<b>60</b>	R	R	R
<b>90</b>	R	R	A
<b>f<sub>2</sub></b>	<b>A (51.6)</b>	<b>A (51.1)</b>	<b>A (51.6)</b>

Table 3.3: MMIP and similarity factor ( $f_2$ ) between the buffers, octanol, and total cumulative percent dissolved using biphasic dissolution with a mixer. A is accepted similarity, R is rejected similarity.

<b>T test</b>	<b>Octa</b>	<b>Buffer</b>	<b>Total</b>
<b>5</b>	0.817	0.009*	0.007*
<b>10</b>	0.828	0.069	0.092
<b>20</b>	0.454	0.156	0.045*
<b>30</b>	0.267	0.624	0.008*
<b>45</b>	0.066	0.525	0.080
<b>60</b>	0.049*	0.594	0.020*
<b>90</b>	0.048*	0.079	0.092

Table 3.4: P values for the biphasic dissolution using a mixer for 5 mM PBS and 10 mM BCB, using a two-tailed t test. \*Indicates a significant difference.

# **Chapter Four**

## **Discussion and Conclusion**



## **4. Discussion**

### **4.1. Intrinsic Dissolution Rate**

The IDR is usually used to study drug dissolution or the effects of residual solvents, and pH effects on the solubility of an active pharmaceutical ingredient.<sup>20,41,44,54,55</sup> Our method of adding a buffer to HCl was performed in order to simulate the physiological environment between the stomach and small intestine following gastric emptying, and to study the effects of the neutralization mechanisms of both buffers.

Undoubtedly, using bicarbonate results in a better IVIVC, but the main drawbacks are reproducibility and hydrodynamic stability when used with bile salts.<sup>10</sup> For this reason, Jantratid et al.<sup>54</sup> and Fuchs et al.<sup>55</sup> recommended the use of maleate as a simulated intestinal buffer, instead of bicarbonate. We aimed to find a method with good reproducibility, that was appropriate for supplying CO<sub>2(g)</sub> without interfering with the hydrodynamics of the media and without creating turbulent flow. Especially when bile salts were used to avoid bubble formation directly at the surface of the drug disk, which would decrease surface area.

#### **4.1.1. Ibuprofen Intrinsic Dissolution Rate**

The curves from all of the experiments show a linear relation, with  $R^2 \sim 1$ . This is essential for being able to measure the slope, then applying Eq. 1.1 to calculate

the IDR. An upward curvature at the end could indicate that an error, such as cracking of the compacted disk, had occurred, which would increase the surface area. When a negative curvature happens, this can indicate that the crystal shape has converted, e.g., changed from amorphous to crystalline form, or another polymorphic form.<sup>20</sup> In our method design, the change in pH could lead to negative curvature; however, this did not happen here, as the IBU solubility decreased at lower pHs. For this reason, and because of the short run time (20 min), IBU showed a linear IDR in all buffers that were used as dissolution media.

Fifty mM PBS is the recommended dissolution medium for IBU in the USP; however, this medium gave a 335% higher IDR than BCB. This indicates that the recommended dissolution buffer for IBU in the USP does not reflect the actual dissolution *in vivo*. The other significant difference appeared when comparing 10 mM PBS to 50 mM PBS, where the difference was 250% higher. This shows the effect of buffer strengths, with a higher buffer strength of PBS resulting in greater dissolution of IBU. As the concentration increases, the buffer capacity also increases, driving the reactions Recs 4.1 and 4.2 to produce salt formation, since more substrate is available for ionizing the IBU (more soluble form), although a similar pH was achieved in both the 10 mM and 50 mM PBS buffers.<sup>56</sup>

The BCB showed a 32% lower IDR when compared to 10 mM PBS, although both have a similar buffer capacity and concentration. This is in agreement with what

had been published by Krieg et al., who obtained the same results, which they ascribed to an irreversible reaction in the BCB at the diffusion layer (Rec 4.3), where it was instantly equilibrated in the case of PBS. They recommended that 4–8 mM PBS should be equivalent to 10 mM BCB. The pH profiles for 10 mM and 50 mM PBS were similar, thus eliminating any effect of pH.<sup>13,57</sup>

Sodium taurocholate and lecithin were used in FaSSIF to simulate small intestine fluid, with sodium taurocholate used at 3 mM and lecithin at 0.75 mM. In a second version (FaSSIF V2), the lecithin was reduced to 0.2 mM at the critical micelle concentration level to produce smaller micelle sizes; the initial results indicated a better IVIVC for the FaSSIF V2.<sup>58–60</sup>

The results of the 50 mM PBBS showed a higher IDR compared to 10 mM PBBS, similar to both media without bile salts (229%). This was expected due to the higher buffering capacity. Also, the BBBS was 25% lower than the 10 mM PBBS, suggesting the same reason for the difference between the BCB and PBS, as the reaction kinetics differed between the two buffers. Taking into account the low concentration of bile salts used, the media with bile salts did not produce any significant differences when compared to the media without bile salts. This is in agreement with Sheng et al. who found that the surfactant did not affect the IDR of low-solubility acidic drugs at high pHs, even when a high concentration was used. These results indicate that the effects of buffer composition and strength play more

important roles than the surfactant in the dissolution media for low-solubility acidic drugs, such as IBU.<sup>61</sup>



#### 4.1.2. Griseofulvin Intrinsic Dissolution Rate

Plotting the cumulative amount over time produced a linear relationship for all of the experiments, with  $R^2 > 0.9$  over 120 min, indicating a successful method design. This was challenging, as a long run time and high rpm were needed to obtain measurable concentrations at the first time point, using the HPLC method described above; however, the long run time and high rpm could cause erosion of the disk surface.<sup>20</sup>

The IDR of GRI in the BCB was 23% higher than in the PSB, but without a statistically significant difference. This is expected for neutral drugs, as they do not form any ions throughout the range of pHs; hence, buffering the pH will not interfere with GRI dissolution.<sup>62</sup> The difference in the pH in the first 15 min resulted from the high speed used for the experiment, where the speed facilitated the escape of  $\text{CO}_2$  from the media.

Adding bile salts to the PBS resulted in a significant increase (38%) in the IDR, which could be attributed to a solubilization effect of the surfactant, leading to an

increase in the partitioning of the GRI to the hydrophobic core in the micelles formed, producing higher drug solubility.

Adding bile salts to the BCB produced a considerable increase in the GRI IDR (106%). As seen with the PBS and PBBS, the increase in the GRI IDR in the presence of bile salts was due to the solubilization ability of the surfactants. Unlike IBU, GRI was not ionized in the experimental pH range, leading to higher micelle partitioning than for ionized drugs, thus the surfactants have a much greater effect.

Also, the BBBS had an 83.3% higher IDR than the PBBS. Small et al. suggested two forms of bile salts micelles – spherical and rod-shaped.<sup>63,64</sup> Zhang et al. studied the effects of salt type on the aggregation of bile salts micelles, finding that the micelle aggregation behavior changed with a change in salts; the rod-like bile salts micelles had a better hydrophobic solubilization ability.<sup>65</sup> More recently, Hildebrand et al. showed that small micelle sizes are associated with a spherical shape, with larger sizes having more complex shapes. Larger micelle sizes in the BBBS indicated that the bile salts in the BCB had a more complex shape, whereas, in the PBS, the micelles were spherical, hence a higher IDR was observed with the BBBS.<sup>66–68</sup>

## 4.2. Biphasic Dissolution

Unlike other systems for low-solubility drugs, biphasic dissolution offers certain similarities to *in vivo* conditions. A drug needs to dissolve in an aqueous medium before it can be absorbed *in vivo*, and this can cause sink conditions. In biphasic dissolution, the drug first dissolves in the buffer, then partitions into the octanol phase, mimicking the sink conditions *in vivo*.<sup>17</sup> Krieg et al. proposed 5 mM PBS as a surrogate buffer for BCB for IBU, but IBU dissolution will change the pH of the medium, as IBU will act as an acid. The buffer capacity of 5 mM PBS is weak and cannot resist this change in pH, and the dissolution of IBU will decrease the pH after some time. Hence, biphasic dissolution is needed in order to study the dissolution of IBU without changing the pH; however, sparging CO<sub>2(g)</sub> into one compartment of the biphasic dissolution system will cause a disturbance in the hydrodynamics of the entire system, as the CO<sub>2(g)</sub> needs to be supplied inside the buffer, with the octanol on top of it.<sup>10,57</sup>

### 4.2.1. Franz Cell Biphasic Dissolution

The Franz cell model was used, as it can separate the aqueous phase (in the main vessel) and the octanol phase (in the Franz cell). This enabled us to add CO<sub>2(g)</sub> above the surface of the buffer in the main vessel; however, the octanol phase showed a notably low amount of dissolved IBU. IBU is highly soluble in octanol (>450

mg/mL).<sup>69</sup> This happened because of the low surface contact area between the octanol and buffer phases, as the contact surface area was limited to the small membrane area, and the flow rate was relatively slow. It takes about 30 min to circulate the entirety of the buffer in the main vessel. Also, the method was not stable; later in the experiment, the membrane broke and octanol appeared in the main vessel. Thus, this method was abandoned, and a two-vessel method with a mixer was developed.

Another interesting result of the Franz cell was the effect of IBU and the pH change. The pH of the buffer was 6.5 before the start of the experiment, and the reported solubility at that pH was 2.7 mg/mL. Then, after the concentration of IBU increased to 0.29 mg/mL, the pH dropped to 6.28, at which point the maximum solubility should have been around 1.7 mg/mL. At the end of the experiment, the pH reached pH 5.9, with 0.45 mg/mL being IBU dissolved; the maximum solubility was 0.7 mg/mL.<sup>70</sup> The high concentration dissolved contradicts sink condition requirements, as 50% of the maximum solubility was reached; however, the relationship between the pH and the amount of IBU dissolved indicated the amount of IBU able to dissolve in the buffer without affecting the pH.

#### **4.2.2. Ibuprofen Biphasic Dissolution Using a Mixer**

Different biphasic protocols were developed in an attempt to enhance the partitioning of the drug by increasing buffer–octanol interface interaction. The buffer could not be mixed with the octanol, otherwise the drug would dissolve in the octanol, rather than dissolving in the buffer; partitioning to the octanol would lead to deceptive dissolution behavior.

#### **4.2.2.1. Partitioning of Ibuprofen**

This was performed in order to study the stability and ability of the system to deliver and mix the buffer effectively with the octanol. The low variability and high octanol partitioning indicate that the system is suitable to be used as a biphasic dissolution setup; however, the total IBU concentration in the system was higher than the limit, possibly due to the slow flow rate (5 mL/min) that means it will take around 50 min for all buffer to circulate through the system. The fact that the total went to 100% after 45 min supports this hypothesis. From the pH profile, the relationship between pH and IBU buffer concentration shows that more than 100 µg/mL of IBU will result in a considerable change in the pH, and this will cause a decrease in the solubility.

#### **4.2.2.2. Ibuprofen Biphasic Dissolution**

##### **4.2.2.2.1. Dissolution in 5 mM Phosphate Buffer**



The early increase in the IBU buffer concentration could be attributed to the same reason as in the partitioning study, where the buffer needed some time to circulate to the octanol phase. This is supported by the maximum time point ( $t_{\max}$ ), as this decreased to 20 min from 45 min when the flow rate was increased to double that used in the partitioning experiment described above. The graph of the octanol partition showed zero-order kinetics, indicating simulation of a successful sink condition. The pH of the buffer was stable throughout the experiment. The highest concentration in the buffer at one point was 84  $\mu\text{g/mL}$ , and the lowest pH was 6.4; this is in agreement with the partitioning study.

#### **4.2.2.2.2. Dissolution in 10 mM Bicarbonate Buffer**

The increase at the beginning of the experiment was expected, due to the above-mentioned reasons, but the steady curve up to 45 min suggests a lower IBU partitioning to the octanol phase, as shown by the flux of IBU in the BCB. The low increase in pH at some points is credited to the effect of the mechanical stress applied by the pumps, as this could facilitate the conversion of  $\text{CO}_{2(\text{aq})}$  to the gas phase; however, this loss was compensated for by applying  $\text{CO}_{2(\text{g})}$  to the surface of the buffer, as was verified by the  $\text{CO}_2$  electrode.

#### **4.2.2.2.3. Biphasic Dissolution Profile Comparison**

Krieg et al. recommended the use of 5 mM PBS as a surrogate for BCB, as it is more convenient to use PBS, it being easier to handle. To compare the two dissolution profiles, the regulatory agencies have recommended certain methods – e.g.,  $f_2$  and the MMIP. A two-tailed t test was applied in order to gain confidence, compared to the MMIP.<sup>13,48</sup>

The buffer showed different IBU dissolution behavior when compared by the MMIP; here, a greater than 10% difference was considered not to be statistically significant. On the other hand, in the octanol phase, similarity was accepted for the first four points, although, after the maximum concentration was reached in the buffer phase, the similarity was rejected. The similarity in the first points could be caused by limitations in the system. The total percentage similarity was rejected for all points, except at the maximum concentration and at the end, when all the drug had been dissolved. This shows the similarity in the extent of dissolved IBU, not the behavior of the dissolution. The extent of the dissolved amount was also shown by similarity in the area under the curve ( $p=0.279$ ). All of these findings suggest that 5 mM PBS is not a good surrogate buffer for 10 mM BCB, as it showed more than a 10% difference in its upper limits. When the percentage difference increased using  $f_2$ , the buffers were similar, as  $f_2$  was 51% in all cases.<sup>47,71</sup>

### **4.3. Conclusions**

This work has demonstrated the importance of using a BCB as a dissolution medium for class II drugs. The higher dissolution of the acidic BCS class II drug IBU in the PBS, compared to the BCB, while having the same ion concentration and buffer capacity, shows the effects of the irreversible reaction kinetics observed with the BCB. This finding is in agreement with Krieg et al. The dissolution of neutral class II drugs in the BBBS, however, was 83% higher than in the PBBS, although the same concentrations were used, suggesting the need to use a BBBS for the dissolution of neutral low-solubility drugs. Furthermore, the sparging of CO<sub>2</sub> above the dissolution medium was a suitable method for maintaining the overall medium pH.

We have shown the differences in the dissolution of IBU in a 10 mM BCB and a 5 mM phosphate buffer, by using a two-compartment biphasic dissolution system and a mixer. Analysis of the two dissolution profiles suggests that the 5 mM PBS is not a good surrogate for the BCB in the case of IBU. Also, the two-compartment system was a suitable method for use as a biphasic dissolution system.

The use of physiologically-relevant buffers showed different dissolution behaviors than in the commonly used PBS. This could be of importance for the assessment of the BCS classes of new drug molecules. Also, using bile salts with a BCB could be of importance for assessing neutral low-solubility drugs for biowaivers. Furthermore, the IVIVC of drug dissolution in BCBs could be

established, which will decrease the costs of drug development and facilitate drug approval through the regulatory agencies.

#### **4.4. Limitations**

Our study was limited to only one model drug of a low-solubility acidic and one neutral drug. Also, the only type of bile salt used was taurocholate; other *in vivo* bile salts were not examined in this study. Furthermore, we did not mimic the complete *in vivo* environment, such as the motility cycle, osmolarity, and enzymic composition of the intestinal juices.

#### **4.5. Future Directions**

The bile salts micelles in the BCB need to be studied in order to determine the shape of the micelles at the same low concentration. Furthermore, the effects of the ionic strength of the buffer on the dissolution of low-solubility neutral drugs in the presence of bile salts need to be studied, as ionic strength can alter the shape of bile salts micelles.

Also, a surrogate phosphate concentration needs to be found, especially when large volumes are needed, or when ionizable drugs are investigated. The surrogate phosphate buffer will need to be tested in the case of enteric-coated tablets, as the BCB showed different dissolution behaviors when compared to the 50 mM

phosphate buffer. Finally, an *in vivo/in vitro* correlation of BCB dissolution, using the current dissolution techniques, needs to be established.

### **References:**

1. Services, H. Guidance for Industry Guidance for Industry Extended Release Oral Dosage Forms : *Evaluation* (1997).
2. Dokoumetzidis, A., Papadopoulou, V. & Macheras, P. Analysis of dissolution data using modified versions of Noyes–Whitney equation and the Weibull function. *Pharm. Res.* **23**, 256–261 (2006).
3. Johnson, K. C. & Swindell, A. C. Guidance in the setting of drug particle size specifications to minimize variability in absorption. *Pharm. Res.* **13**, 1795–1798 (1996).
4. Lu, Y., Kim, S. & Park, K. In vitro-in vivo correlation: Perspectives on model development. *Int. J. Pharm.* **418**, 142–148 (2011).
5. Fuchs, A. & Dressman, J. B. Composition and physicochemical properties of fasted-state human duodenal and jejunal fluid: A critical evaluation of the

- available data. *J. Pharm. Sci.* **103**, 3398–3411 (2014).
6. Kalantzi, L. *et al.* Characterization of the human upper gastrointestinal contents under conditions simulating bioavailability/bioequivalence studies. *Pharm. Res.* **23**, 165–176 (2006).
  7. McConnell, E. L., Fadda, H. M. & Basit, A. W. Gut instincts: Explorations in intestinal physiology and drug delivery. *Int. J. Pharm.* **364**, 213–226 (2008).
  8. Fadda, H. M., Merchant, H. A., Arafat, B. T. & Basit, A. W. Physiological bicarbonate buffers : stabilisation and use as dissolution media for modified release systems. **382**, 56–60 (2009).
  9. Mcnamara, D. P., Whitney, K. M. & Goss, S. L. Use of a Physiologic Bicarbonate Buffer System for Dissolution Characterization of Ionizable Drugs. **20**, 2–7 (2003).
  10. Boni, J. E., Brickl, R. S. & Dressman, J. Is bicarbonate buffer suitable as a dissolution medium ? 1375–1382 (2007). doi:10.1211/jpp.59.10.0007
  11. Liu, F., Merchant, H. A., Kulkarni, R. P., Alkademi, M. & Basit, A. W. European Journal of Pharmaceutics and Biopharmaceutics Evolution of a physiological pH 6 . 8 bicarbonate buffer system : Application to the dissolution testing of enteric coated products. *Eur. J. Pharm. Biopharm.* **78**, 151–157 (2011).
  12. Sheng, J. J., McNamara, D. P. & Amidon, G. L. Toward an in vivo

- dissolution methodology: a comparison of phosphate and bicarbonate buffers. *Mol. Pharm.* **6**, 29–39 (2009).
13. Krieg, B. J., Taghavi, S. M., Amidon, G. L. & Amidon, G. E. In Vivo Predictive Dissolution : Comparing the Effect of Bicarbonate and Phosphate Buffer on the Dissolution of Weak Acids and Weak Bases. *J. Pharm. Sci.* **104**, 2894–2904 (2015).
  14. Phillips, D. J., Pygall, S. R., Cooper, V. B. & Mann, J. C. Overcoming sink limitations in dissolution testing: A review of traditional methods and the potential utility of biphasic systems. *J. Pharm. Pharmacol.* **64**, 1549–1559 (2012).
  15. Wurster, D. E. & Polli, G. P. Investigation of drug release from solids IV. Influence of adsorption on the dissolution rate. *J. Pharm. Sci.* **50**, 403–406 (1961).
  16. Reese, D. R., Irwin, G. M., Dittert, L. W., Chong, C. W. & Swintosky, J. V. Drug Partitioning I. *J. Pharm. Sci.* **53**, 591–597 (1964).
  17. Levy, G., Leonards, J. R. & Procknal, J. A. Development of in vitro dissolution tests which correlate quantitatively with dissolution rate-limited drug absorption in man. *J. Pharm. Sci.* **54**, 1719–1722 (1965).
  18. Niebergall, P. J., Patil, M. Y. & Sugita, E. T. Simultaneous determination of dissolution and partitioning rates in vitro. *J. Pharm. Sci.* **56**, 943–947 (1967).

19. Jamzad, S. & Fassihi, R. Role of surfactant and pH on dissolution properties of fenofibrate and glipizide--a technical note. *AAPS PharmSciTech* **7**, E33 (2006).
20. Convention, U. S. P. *United States Pharmacopeia and National Formulary (USP 36-NF 31). Vol 1.* (2012).
21. Alli, D., Bolton, S. & Gaylord, N. G. Hydroxypropylmethylcellulose–anionic surfactant interactions in aqueous systems. *J. Appl. Polym. Sci.* **42**, 947–956 (1991).
22. Daly, P. B., Davis, S. S. & Keimerley, J. W. The effect of anionic surfactants on the release of chlorpheniramine from a polymer matrix tablet. *Int. J. Pharm.* **18**, 201–205 (1984).
23. Liu, C., Desai, K. G. H., Tang, X. & Chen, X. Solubility of rofecoxib in the presence of aqueous solutions of glycerol, propylene glycol, ethanol, Span 20, Tween 80, and sodium lauryl sulfate at (298.15, 303.15, and 308.15) K. *J. Chem. Eng. Data* **50**, 2061–2064 (2005).
24. Walkling, W. D., Nayak, R. K., Plostnieks, J. & Cressman, W. A. A partially organic dissolution medium for griseofulvin dosage forms. *Drug Dev. Ind. Pharm.* **5**, 17–27 (1979).
25. Brown, W. Apparatus 4 flow through cell: some thoughts on operational characteristics. *Dissolution Technol* **12**, 28–30 (2005).



26. Kakhi, M. Classification of the flow regimes in the flow-through cell. *Eur. J. Pharm. Sci.* **37**, 531–544 (2009).
27. Qureshi, S. A. *et al.* Application of flow-through dissolution method for the evaluation of oral formulations of nifedipine. *Drug Dev. Ind. Pharm.* **20**, 1869–1882 (1994).
28. Gabriëls, M. & Plaizier-Vercammen, J. Design of a dissolution system for the evaluation of the release rate characteristics of artemether and dihydroartemisinin from tablets. *Int. J. Pharm.* **274**, 245–260 (2004).
29. Locher, K., Borghardt, J. M., Frank, K. J., Kloft, C. & Wagner, K. G. Evolution of a mini-scale biphasic dissolution model: Impact of model parameters on partitioning of dissolved API and modelling of in vivo-relevant kinetics. *Eur. J. Pharm. Biopharm.* **105**, 166–175 (2016).
30. Pestieau, A. & Evrard, B. In vitro biphasic dissolution tests and their suitability for establishing in vitro-in vivo correlations: A historical review. *Eur. J. Pharm. Sci.* **102**, 203–219 (2017).
31. Theis, D. L., Lucisano, L. J. & Halstead, G. W. Use of Stable Isotopes for Evaluation of Drug Delivery Systems: Comparison of Ibuprofen Release in Vivo and in Vitro from Two Biphasic Release Formulations Utilizing Different Rate-Controlling Polymers. *Pharmaceutical Research: An Official Journal of the American Association of Pharmaceutical Scientists* **11**, 1069–

- 1076 (1994).
32. Tsume, Y., Igawa, N., Drelich, A. J., Amidon, G. E. & Amidon, G. L. The Combination of GIS and Biphasic to Better Predict In Vivo Dissolution of BCS Class Iib Drugs, Ketoconazole and Raloxifene. *J. Pharm. Sci.* **107**, 307–316 (2018).
  33. Xu, H., Shi, Y., Vela, S., Marroum, P. & Gao, P. Developing Quantitative In Vitro–In Vivo Correlation for Fenofibrate Immediate-Release Formulations With the Biphasic Dissolution-Partition Test Method. *J. Pharm. Sci.* **107**, 476–487 (2018).
  34. A Theoretical Basis for a Biopharmaceutic Drug Classification- The Correlation of in Vitro Drug Product Dissolution and in Vivo Bioavailability.pdf.
  35. Administration, F. and D. Guidance for industry: waiver of in vivo bioavailability and bioequivalence studies for immediate-release solid oral dosage forms based on a biopharmaceutics classification system. *Food Drug Adm. Rockville, MD* (2000).
  36. Agency, E. M. Committee for Medicinal Products for Human Use: Guideline on similar biological medicinal products containing biotechnology-derived proteins as active substance: non-clinical and clinical issues. (2013).
  37. World Health Organization. WHO expert committee on specifications for

- pharmaceutical preparations. Annex 7 Multisource (generic) pharmaceutical products: guidelines on registration requirements to establish interchangeability. *WHO Tech. Rep. Ser. 937, Inf. 40* **7**, 461 (2006).
38. Wood, J. H., Syarto, J. E. & Letterman, H. Improved holder for intrinsic dissolution rate studies. *J. Pharm. Sci.* **54**, 1068 (1965).
  39. Issa, M. G. & Ferraz, H. G. Intrinsic dissolution as a tool for evaluating drug solubility in accordance with the biopharmaceutics classification system. *Dissolution Technol.* **18**, 6–13 (2011).
  40. Avdeef, A. & Tsinman, O. Miniaturized rotating disk intrinsic dissolution rate measurement: Effects of buffer capacity in comparisons to traditional wood's apparatus. *Pharm. Res.* **25**, 2613–2627 (2008).
  41. Tseng, Y. C., Patel, M. & Zhao, Y. Determination of intrinsic dissolution rate using miniaturized rotating and stationary disk systems. *Dissolution Technol.* **21**, 24–29 (2014).
  42. Andersson, S. B. E. *et al.* Interlaboratory Validation of Small-Scale Solubility and Dissolution Measurements of Poorly Water-Soluble Drugs. *J. Pharm. Sci.* **105**, 2864–2872 (2016).
  43. Berger, C. M. *et al.* Technical note: Miniaturized intrinsic dissolution rate (Mini-IDR<sup>TM</sup>) measurement of griseofulvin and carbamazepine. *Dissolution Technol.* **14**, 39–41 (2007).

44. Yu, L. X., Carlin, A. S., Amidon, G. L. & Hussain, A. S. Feasibility studies of utilizing disk intrinsic dissolution rate to classify drugs. *Int. J. Pharm.* **270**, 221–227 (2004).
45. Ifegwu, O. C., Anyakora, C., Chigome, S. & Torto, N. Analytical Chemistry Insights. 17–25 (2014). doi:10.4137/ACI.S13560.Received
46. Trotta, M., Gallarate, M., Carlotti, M. E. & Morel, S. Preparation of griseofulvin nanoparticles from water-dilutable microemulsions. *Int. J. Pharm.* **254**, 235–242 (2003).
47. Yoshida, H., Shibata, H., Izutsu, K.-I. & Goda, Y. Comparison of dissolution similarity assessment methods for products with large variations:  $t^2$ -statistics and model-independent multivariate confidence region procedure for dissolution profiles of multiple oral products. *Biol. Pharm. Bull.* **40**, 722–725 (2017).
48. FDA. Guidance for Industry Dissolution Testing of Immediate. *Evaluation* **4**, 15–22 (1997).
49. Zhang, Y. *et al.* DDSolver: An Add-In Program for Modeling and Comparison of Drug Dissolution Profiles. *AAPS J.* **12**, 263–271 (2010).
50. Saranadasa, H. & Krishnamoorthy, K. A multivariate test for similarity of two dissolution profiles. *J. Biopharm. Stat.* **15**, 265–278 (2005).
51. Yuwono, M. & Indrayanto, G. Validation of chromatographic methods of

- analysis. *Profiles Drug Subst. Excipients Relat. Methodol.* **32**, 243–259 (2005).
52. Colin Cameron, A. & Windmeijer, F. A. G. An R-squared measure of goodness of fit for some common nonlinear regression models. *J. Econom.* **77**, 329–342 (1997).
53. Buncl, E. & Rajagopal, S. Solvatochromism and solvent polarity scales. *Acc. Chem. Res.* **23**, 226–231 (1990).
54. Dezani, A. B., Pereira, T. M., Caffaro, A. M., Reis, J. M. & Serra, C. H. dos R. Equilibrium solubility versus intrinsic dissolution: Characterization of lamivudine, stavudine and zidovudine for BCS classification. *Brazilian J. Pharm. Sci.* **49**, 853–863 (2013).
55. Shekunov, B. & Montgomery, E. R. Theoretical Analysis of Drug Dissolution: I. Solubility and Intrinsic Dissolution Rate. *J. Pharm. Sci.* **105**, 2685–2697 (2016).
56. Levis, K. A., Lane, M. E. & Corrigan, O. I. Effect of buffer media composition on the solubility and effective permeability coefficient of ibuprofen. *Int. J. Pharm.* **253**, 49–59 (2003).
57. Krieg, B. J., Taghavi, S. M., Amidon, G. L. & Amidon, G. E. In vivo predictive dissolution: Transport analysis of the CO<sub>2</sub>, bicarbonate in vivo buffer system. *J. Pharm. Sci.* **103**, 3473–3490 (2014).

58. Williams, H. D. *et al.* Strategies to Address Low Drug Solubility in Discovery and Development. *Pharmacol. Rev.* **65**, 315–499 (2013).
59. Karlsson, E. *et al.* articles Simulating Fasted Human Intestinal Fluids : Erik So. *Mol. Pharm.* **7**, 1498–1507 (2010).
60. Lehto, P. *et al.* Use of conventional surfactant media as surrogates for FaSSIF in simulating in vivo dissolution of BCS class II drugs. *Eur. J. Pharm. Biopharm.* **78**, 531–538 (2011).
61. Sheng, J. J., Kasim, N. A., Chandrasekharan, R. & Amidon, G. L. Solubilization and dissolution of insoluble weak acid, ketoprofen: Effects of pH combined with surfactant. *Eur. J. Pharm. Sci.* **29**, 306–314 (2006).
62. Avdeef, A. Physicochemical Profiling (Solubility, Permeability and Charge State). *Curr. Top. Med. Chem.* **1**, 277–351 (2001).
63. Small, D. M., Penkett, S. A. & Chapman, D. D. m. small\*\*, s. a. penkett. **176**, 178–189 (1969).
64. Carey, M. C. Micelle Formation by Bile Salts. *Arch. Intern. Med.* **130**, 506 (1972).
65. Zhang, S. Z., Xie, J. W. & Liu, C. S. Microenvironmental properties and chiral discrimination abilities of bile salt micelles by fluorescence probe technique. *Anal. Chem.* **75**, 91–97 (2003).
66. Hildebrand, A., Garidel, P., Neubert, R. & Blume, A. Thermodynamics of

- Demicellization of Mixed Micelles Composed of Sodium Oleate and Bile Salts. 320–328 (2004). doi:10.1021/la035526m
67. Garidel, P., Hildebrand, A., Neubert, R. & Blume, A. Thermodynamic Characterization of Bile Salt Aggregation Isothermal Titration Calorimetry. 5267–5275 (2000). doi:10.1021/la9912390
68. Subuddhi, U. & Mishra, A. K. Micellization of bile salts in aqueous medium: A fluorescence study. *Colloids Surfaces B Biointerfaces* **57**, 102–107 (2007).
69. Filippa, M. A. & Gasull, E. I. Ibuprofen solubility in pure organic solvents and aqueous mixtures of cosolvents: Interactions and thermodynamic parameters relating to the solvation process. *Fluid Phase Equilib.* **354**, 185–190 (2013).
70. Calculation, C.-I. C. S. ChemAxon, Ltd: 2016.
71. Approach, T. P. & Approaches, N. Comparison of dissolution profile by Model independent & Model dependent methods. **2**,

